TRANSPORTATION RESEARCH RECORD

507

Formerly issued as Highway Research Record

Bridge Design

6 reports prepared for the 53rd Annual Meeting of the Highway Research Board

subject area

27 bridge design

TRB

TRANSPORTATION RESEARCH BOARD

NATIONAL RESEARCH COUNCIL

Washington, D. C., 1974

NOTICE

These papers report research work of the authors that was done at institutions named by the authors. The papers were offered to the Transportation Research Board of the National Research Council for publication and are published here in the interest of the dissemination of information from research, one of the major functions of the Transportation Research Board.

Before publication, each paper was reviewed by members of the TRB committee named as its sponsor and accepted as objective, useful, and suitable for publication by the National Research Council. The members of the review committee were chosen for recognized scholarly competence and with due consideration for the balance of disciplines appropriate to the subject concerned.

Responsibility for the publication of these reports rests with the sponsoring committee. However, the opinions and conclusions expressed in the reports are those of the individual authors and not necessarily those of the sponsoring committee, the Transportation Research Board, or the National Research Council.

Each report is reviewed and processed according to the procedures established and monitored by the Report Review Committee of the National Academy of Sciences. Distribution of the report is approved by the President of the Academy upon satisfactory completion of the review process.

The National Research Council is the principal operating agency of the National Academy of Sciences and the National Academy of Engineering, serving government and other organizations. The Transportation Research Board evolved from the 54-year-old Highway Research Board. The TRB incorporates all former HRB activities but also performs additional functions under a broader scope involving all modes of transportation and the interactions of transportation with society.

Transportation Research Record 507
International Standard Book Number 0-309-02350-5
Library of Congress Catalog Card Number 74-29184
Price: $3.40

Transportation Research Board publications may be ordered directly from the Board. They are also obtainable on a regular basis through organizational or individual supporting membership in the Board; members or library subscribers are eligible for substantial discounts. For further information write to the Transportation Research Board, National Academy of Sciences, 2101 Constitution Avenue N.W., Washington, D.C. 20418.

Transportation Research Record 507 was edited for Transportation Research Board by Joan B. Silberman.

CONTENTS

FOREWORD iv

PUBLIC RESPONSE TO BRIDGE COLORS
William Zuk 1

ANALYSIS CHARTS FOR ISSUING VEHICLE PERMITS
Conrad P. Heins, Jr., and Richard C. Forbes 6

COMPARISON OF MEASURED AND COMPUTED LOAD-DEFLECTION BEHAVIOR OF TWO HIGHWAY BRIDGES
Edwin G. Burdette, David W. Goodpasture, and Stephen K. Doyle 17

ASSESSMENT OF FATIGUE LIFE OF A STEEL GIRDER BRIDGE IN SERVICE
Fernando Cicci and Paul Csagoly 26

BRIDGE FATIGUE DUE TO DAILY TRAFFIC
Conrad P. Heins, Jr., and C. F. Galambos 45

NEW PROCEDURE FOR FATIGUE DESIGN OF HIGHWAY BRIDGE GIRDERS
Fred Moses and Robert Garson 58

SPONSORSHIP OF THIS RECORD 68

FOREWORD

The six papers in this RECORD are of special interest to the highway bridge designer. The papers are timely and report on important areas in bridge design.

Zuk discusses the results of a survey about preferred bridge colors and their effect on (a) a random sampling of motorists, (b) residents in the area of the test bridge site, and (c) people with professional training in the arts. All groups generally preferred the lighter colors to the darker colors, and the author recommends that highway departments make more use of popular colors in view of their aesthetic value and public preference.

Heins and Forbes address the problem confronting highway departments in issuing permits for overloads. They develop simple and closely approximate procedures for appraising a structure's capacity to carry a specified overload under controlled conditions without damaging the structure. Their work should be of value to those divisions of highway departments responsible for issuing overload permits.

The paper by Burdette, Goodpasture, and Doyle discusses the load-deflection test results of two continuous deck girder bridges. A four-span structure was designed with shear study connectors to provide composite action, and a three-span structure was designed without any provision for shear development between the deck and steel beams. The test results of the load-deflection curves agreed closely with the theoretically calculated values for both structures and were particularly close for the four-span structure with shear stud connectors.

Cicci and Csagoly address live-load stress development under normal traffic in 200 hours of recording measurement in a steel girder structure with welded cover plates. The results from the strain gauges placed in critical locations showed that the live-load peak stress reached 4,000 psi only once in 10 hours, a value that is less than 50 percent of the design live-load stress. The authors conclude that fatigue distress is precluded with these low stresses at such infrequent occurrences.

Heins and Galambos present a loading history of bridge studies in the past 5 years. Their data that live-load stresses are generally low agree with the findings of Cicci and Csagoly, and they further recommend revisions for currently adopted fatigue design criteria. This paper describes one possible method of fatigue design.

Moses and Garson also recognize the low stress levels reported in numerous bridge loading history studies and propose a method for predicting fatigue life that can be easily incorporated into the design of bridge girders. Their procedure is based on a probabilistic load model that forecasts histograms of highway bridge loading. Several examples of fatigue design are included.

—H. L. Kinnier

PUBLIC RESPONSE TO BRIDGE COLORS

William Zuk, Virginia Highway Research Council and
University of Virginia

Two test bridges were selected in Charlottesville, Virginia, to determine people's reactions to bridges covered with white, yellow, green, blue, red, brown, black, or aluminum-colored paint. One bridge was painted a different color each month, and the other was kept the same color for comparison. After each painting, interviews were held with (a) motorists seeing the bridges, (b) persons living near the bridges, and (c) people with formal aesthetic training. More than 1,300 interviews were held for the 10 different bridge colors. The results show that white, yellow, light blue, and green are definitely preferred over brown, black, and aluminum by all groups. Red and dark blue were liked by aesthetically trained people; others thought less highly of them. On the basis of this study, it is recommended that more extensive use of popular colors be considered for highway bridges in the United States. A technique to aid in making a color selection for any given bridge has been developed to photographically color-alter the picture of a bridge so that color comparisons can be easily and inexpensively made.

•A STEEL bridge in Charlottesville, Virginia, was selected to be painted different colors to determine people's responses to these colors. The bridge selected was the Locust Avenue bridge (Fig. 1) over the Charlottesville bypass (US-250). Within a few blocks of Locust Avenue along the same highway heading west is a similar bridge on Park Street (Fig. 2), which was used as a control bridge. Throughout the study the Park Street bridge remained the same color, light green. A traffic light is located just west of the Park Street bridge, which allowed for convenient interviewing of motorists viewing the two bridges when they stopped at the red signal.

Three different groups of people were interviewed about their color preferences for these bridges. Group A included a random sampling of motorists and vehicle occupants who just viewed the bridges. During such interviewing, a large sign was placed east of the Locust Avenue bridge on the bypass to alert travelers that a bridge color survey was under way and ask them to take note of the colors of the two bridges. Group B included people who lived near the bridges. It was believed that such people, feeling that the bridges were a permanent part of their neighborhood and that they therefore were more personally concerned, would represent a different point of view from transient motorists. Group C was made up of people with professional training in the arts, such as artists, architects, and landscape architects.

PAINTINGS AND RESPONSES

In September 1972, the eastern face of the steel girder on the Locust Avenue bridge (originally light green) was painted its first color, white (No. 17886) (1).

Because the older surface paint on the Park Street bridge appeared shabby in comparison with the fresh paint on the Locust Avenue bridge, it was decided to repaint the eastern face of the steel girder on that bridge as well. This was painted light green (No. 14533) to approximate the original color of the Locust Avenue bridge.

Surveys of the three groups described previously were then begun. For group A (the motorists) only quick interviews were made while they were stopped at the traffic

Publication of this paper sponsored by Committee on General Structures.

Figure 1. Locust Avenue bridge.

Figure 2. Park Street bridge.

Table 1. Survey results.

Groups	No. Interviewed			Age of Interviewees (percent)			Preference[a] (percent)			
	Male (percent)	Female (percent)	Total	0-25	26-50	51-75	Like	Evenly Divided	Dislike	Indifferent
A (motorists)	78	22	131	36	58	6	57	14	25	4
B (residents)	38	62	26	31	42	27	42	12	42	4
C (artistically trained)	89	11	18	61	39	0	72	22	6	0

[a]Compared to light green.

Figure 3. Color preference chart.

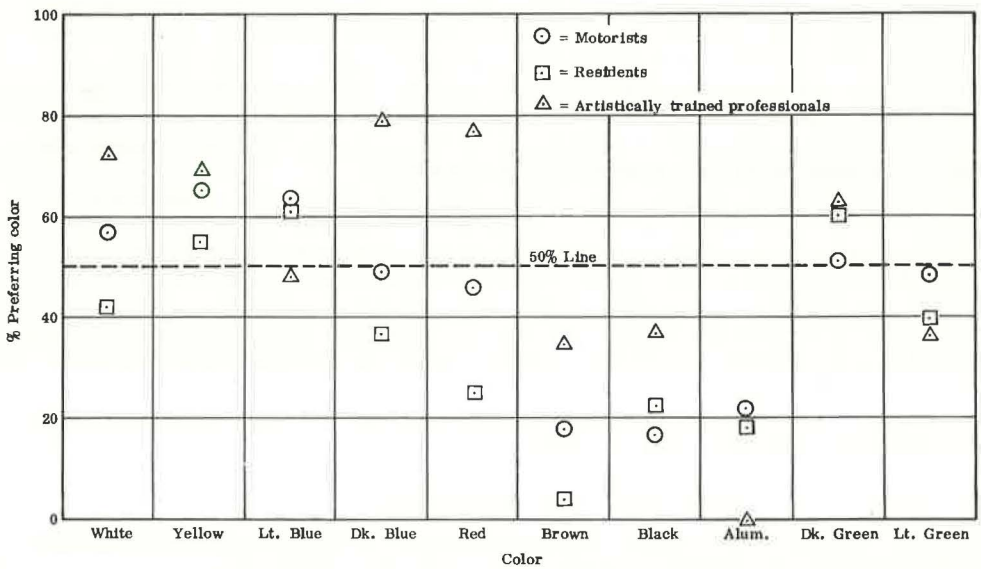

signal. The interviewers mainly obtained color preference on the Locust Avenue and Park Street bridges. Interviews of the other groups were more extensive and allowed for general comments regarding the color. Table 1 gives results of the survey for white. Group A (motorists) felt that white was highly visible; truck drivers especially liked it. Group B (residents) felt that white presented a nice clean look although it might soil easily. Group C (artistically trained) felt that white was satisfactory but that other colors were preferable.

At about 1-month intervals, the Locust Avenue bridge was repainted another color and surveys were taken again. The sequence of colors was yellow (No. 13538), light blue (No. 15200), dark blue (No. 15050), red (No. 11105), brown (No. 10091), black (No. 17038), aluminum (No. 17178), and dark green (No. 14062). Tables for these colors (similar to Table 1) are not shown for the sake of brevity, but they are available from the author on request.

ANALYSIS AND CONCLUSIONS

The data are obviously subject to many interpretations. The percentage of people in each of the three groups who prefer a particular bridge color is shown in Figure 3. Because of the comparative technique used in the study in which each bridge color was compared with light green (standard), the preference for the standard color had to be arrived at by inference. An overwhelming number of comments by those interviewed who responded that their preference for the light green and dark green was almost the same showed that those who were evenly divided between the two colors and those who disliked the dark green as opposed to the light green were considered as preferring light green.

For purposes of further division, a 50 percent line is drawn across Figure 3 that separates the more popular from the less popular colors at a glance. Group A (motorists) preferred white, yellow, light blue, and dark green; these colors are closely followed by dark blue, light green, and red. Group B (residents) preferred yellow, light blue, and dark green; these colors are closely followed by white and light green. Group C (aesthetically trained professionals) preferred white, yellow, dark blue, red, and dark green; these colors were followed closely by light blue. Brown, black, and aluminum were unpopular with all groups.

Figure 3 shows that preferences of groups A and B do not differ significantly; this suggests that whatever colors are acceptable to transient motorists are also acceptable to persons who live near the bridge and consider it as part of their permanent neighborhood environment. But, as expected, the opinions of group C vary somewhat with those of groups A and B. Whereas yellow and dark green are liked by all groups, group C has a strong preference for dark blue and red.

Color preference is a subtle determination that is subject to time, place, mood, fashion, past association, and the like; however, it can be concluded that the interviewees would, by and large, be receptive to bridges painted different colors.

A small percentage felt that no extra money should be spent painting bridges different colors. There are also some who are not particularly aware of the color of bridges at all and would accept any reasonable color.

A great deal of quantitative information (1 through 12) is available on color and its effect on people; however, none applies to bridge structures. Universally, if any one color is more popular than any other, it is blue (2). This study shows that blue is indeed popular, but that, for bridges, other colors are liked as well. Many states already are using bridge colors other than the standard aluminum and green such as blue, yellow, white, red, and maroon.

METHOD FOR SELECTING BRIDGE COLOR

The following relatively inexpensive procedure is proposed to provide a rational method for selecting bridge colors. It is based on the hypothesis that opinions from a group of people are apt to be more acceptable than an opinion from a single "expert." The method involves altering the bridge color by photographic means rather than by actually painting the bridge as was done in this study. This way, the bridge color can

be evaluated by a random or selected group of people conveniently and efficiently by viewing a series of colored slides or prints of the same bridge in different colors. It is recommended that the color of each bridge be considered individually in relation to its specific site and unique features. No one color suits all conditions.

For older bridges requiring repainting, photographs of these bridges can be taken as is, including their actual background or setting. For new bridges, the selection of the final paint color should be deferred until bridge construction is essentially complete. The color-altering process to be described can be accomplished in but a few days, which will not significantly delay the full completion of any new bridge.

The process is basically the same for all bridge types and colors but is modified somewhat depending on darkness of the original color of the bridge in question. These original colors will be classified as light (aluminum, white, yellow, etc.), medium (light or medium green, blue, orange, etc.), and dark (black, rust, etc.).

The following color-altering photographic technique has been developed, tried, and tested at the Virginia Highway Research Council for a variety of bridge types and colors and has been found to be quite realistic.

1. Photograph the bridge on outdoor color slide film.
2. Develop an 8- by 10-in. (20 by 25 cm) color print from the slide or slides selected. (The print should be of good quality.)
3. For light and medium original bridge colors, photographically reverse the color slide. (For dark original bridge colors, this step may be omitted.)
4. From the black and white negative, enlarge a number of black and white prints of the section of the bridge that will be color-altered. The enlargement must correspond exactly in size with the 8- by 10-in. (20 by 25 cm) color print. This can be done by placing the color print under the enlarger and carefully lining up the black and white negative projection with the color print. For originally dark bridges, project the original color negative onto black and white paper to produce the reverse black and white tones.
5. For originally light or dark bridges, apply colored transparent overlays of plastic acetate onto the black and white sections to be color-altered. (Commercially available zip-a-tone rub-on overlays are available in 144 different colors.) For originally medium-colored bridges, black and white prints must be colored with photographic oil paints or tints that are commercially available. For best results with oils, the black and white print should be on rough mat surface paper.
6. Carefully cut out the color-altered section of the black and white print, darken the cut white edges of the paper, and place this section (a bridge beam for example) on the corresponding section of the 8- by 10-in. (20 by 25 cm) color print.
7. With the color slide film, photograph the 8- by 10-in. (20 by 25 cm) print with the added color-altered section. Repeat this step, with as many different color-altered sections as desired.
8. Process the film used in step 7 for use as colored slides, colored prints, or both.

ACKNOWLEDGMENTS

In addition to acknowledging the general support and funding of this study provided by Jack H. Dillard and Wallace T. McKeel, Jr., of the Virginia Highway Research Council, I would like to thank the following people for their special assistance: Guy B. Agnor, Jr., Director of Public Works for the City of Charlottesville; Walter Lumpp, painting contractor; Wayne Tucker, student assistant; and Paul Hughes and Christopher Zuk, photographers. Finally, appreciation is extended to the many hundreds of people who helpfully responded to the interviews conducted in this study.

REFERENCES

1. Colors. Federal Standard No. 595a, Vol. 1, General Services Administration, Washington, D.C., 1968.
2. Munro, T. Toward Science in Aesthetics. Liberal Arts Press, New York, 1956.
3. Jacobson, E. Basic Color. Theobald Press, Chicago, 1948.

4. Gatz, K., and Wallenfang, W. Color in Architecture. Reinhold, New York, 1961.
5. Faulkner, W. Architecture and Color. John Wiley, New York, 1972.
6. Judd, D. B., and Wyszecki, G. Color in Business, Science, and Industry, 2nd Ed. John Wiley, New York, 1963.
7. Wilson, R. F. Color in Industry Today. Macmillan, New York, 1960.
8. Munsell Book of Color. Munsell Color Company, Baltimore, 1929.
9. Ostwald, W. Color Science. Windson and Newton, London, 1931.
10. Steel Structures Painting Manual. Steel Structures Painting Council, Vols. 1 and 2, Pittsburgh, 1957.
11. Protective Coatings for Highway Structural Steel. NCHRP Rept. 74, 1969.
12. Zuk, W. A Methodology for Evaluating the Aesthetic Appeal of Bridge Designs. Highway Research Record 428, 1973 pp. 1-4.

ANALYSIS CHARTS FOR ISSUING VEHICLE PERMITS

Conrad P. Heins, Jr., and Richard C. Forbes,
College of Engineering, University of Maryland

A methodology that can be used to ascertain the safety of continuous (two- and three-span) composite girder slab bridges under heavy vehicle (permit) loads is discussed. The method [designed according to the 1969 AASHO code (2)] has been used for developing a series of charts, which predict directly whether a given permit vehicle causes an overstress condition in a given structure. The criteria for safety of the structure are based on the primary moment in the girders and are governed by the girder steel stress. Typical permit vehicles that meet the safety requirements have also been determined.

•THE transport of heavy loads through Maryland requires special vehicles and road permits. Issuance of these permits can only be granted when the travel route, which in most instances contains bridges, has been investigated. The safety of these bridge structures can only be assured by carefully analyzing or rating these various bridges for the proposed loads. These analyses require time that often is not available because the permit requests are generally required immediately or on weekends. The personnel issuing the permits are not engineers; therefore, guidance from the Maryland State Highway Administration bridge section personnel is imperative.

A series of analysis charts were developed (1) to reduce the required investigating time by the bridge engineer and to assure that the issuance of permits can be performed quickly and efficiently. These charts can be used by the permit office (with some guidance) in selecting the proper truck route and issuing permits.

The charts that were developed are limited to two- and three-span prismatic continuous bridges of the following lengths:

1. Two span, 70 ft ≤ L ≤ 140 ft and
2. Three span, in which the center span is 70 ft ≤ L ≤ 140 ft and the end span is 70 ft ≤ NL ≤ 140 ft where 0.5 ≤ N ≤ 1.0.

The charts were developed in accordance with the procedures used by the Maryland State Highway Administration and the AASHO code. In particular, the following design criteria were used:

1. Distribution of wheel loads according to S/7.0, where S = girder spacing;
2. Impact of 5 percent; and
3. Steel beam stresses not exceeding 0.75 Fy, where Fy = minimum yield strength.

In issuing the permit, the following restrictions are followed:

1. No other vehicles are allowed on the bridge when the permit vehicles are crossing it,
2. The speed is restricted to a crawl (3 to 4 mph), and
3. The permit vehicle should travel down the middle of the bridge in line with the main girders.

VEHICLE TYPES

The induced girder moments caused by each of these vehicles must be examined so that charts that reflect the load effects of all present permit vehicles may be developed.

Publication of this paper sponsored by Committee on General Structures.

Determination of these girder moments first required the examination of the characteristics of 250 vehicles that were issued permits by the Maryland State Highway Administration. These vehicles had gross weights from 65 to 1,017 kips and lengths from 18.5 to 129.6 ft.

The vehicles were classified into twelve types (Figs. 1 through 3) according to the number of axles. Characteristics of these particular trucks will not exceed allowable bridge stresses and will satisfy allowable chart conditions.

GIRDER MOMENTS

Classifying the permit vehicles by axle number eliminates one independent variable. The other variables considered are wheelbase and gross weight. Comparisons between these variables and induced girder moments (M_{PV}) caused by these permit vehicles have shown that the primary variable is gross weight GW (1). A plot of the induced moment divided by gross weight MGW plotted against span length produced a straight line with scatter about the mean line. The mean equation is found by a linear regression analysis of the data with the scatter prescribed by the deviation 2S. Figure 4 shows a plot of the moments induced at the support and midspan of a two-span structure and moment at the support of a three-span structure for N = 1.0 and 0.9. Similar trends occurred for all other plots.

The induced girder moments caused by the permit trucks were obtained by using computerized influence lines (1, 3). Similar moments were obtained because of AASHO vehicle design loads.

General moment equations have been determined (1) for the permit vehicle and AASHO truck loads. These equations are of the form:

$$M_{PV} = (A + B \cdot L + 2S)\, GW \tag{1}$$

$$M_{AASHO} = (C + D \cdot L)\, 72.0 \tag{2}$$

where

A, B, C, D = coefficients obtained from regression analysis,
S = standard deviation,
L = span length, and
72.0 = vehicle GW.

A wheel-load distribution must be used to account for the interaction of the girders in a system. Therefore, the induced girder moments (Eqs. 1 and 2) are modified as follows:

$$M_{PV} = \frac{M_{PV}}{2} \times \frac{S}{7.0} \tag{3}$$

$$M_{AASHO} = \frac{M_A}{2} \times \frac{S}{5.5} \tag{4}$$

The half factor accounts for the wheel-load effect, because gross weight is used in Eqs. 1 and 2. S/7.0 and S/5.5 are the wheel-load distribution factors, and S is the girder spacing. Ratio R of these equations is

$$R = \frac{M_{PV}}{M_A} \tag{5}$$

or

$$R = \frac{[A + B \cdot L + 2S]\, \frac{GW}{2}\, \frac{S}{7.0}}{[C + D \cdot L]\, \frac{72.0}{2}\, \frac{S}{5.5}} \tag{6}$$

Figure 1. Typical trucks: types 2, 3, 4, and 5.

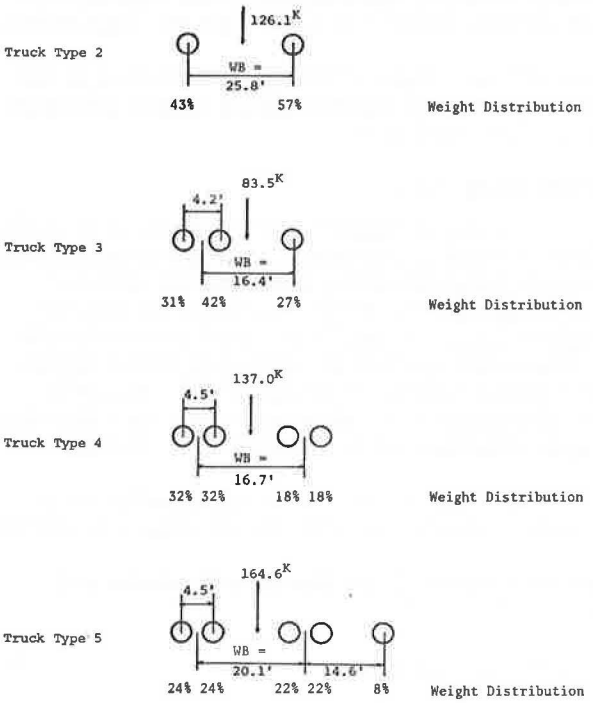

Figure 2. Typical trucks: types 6, 7, 8, and 9.

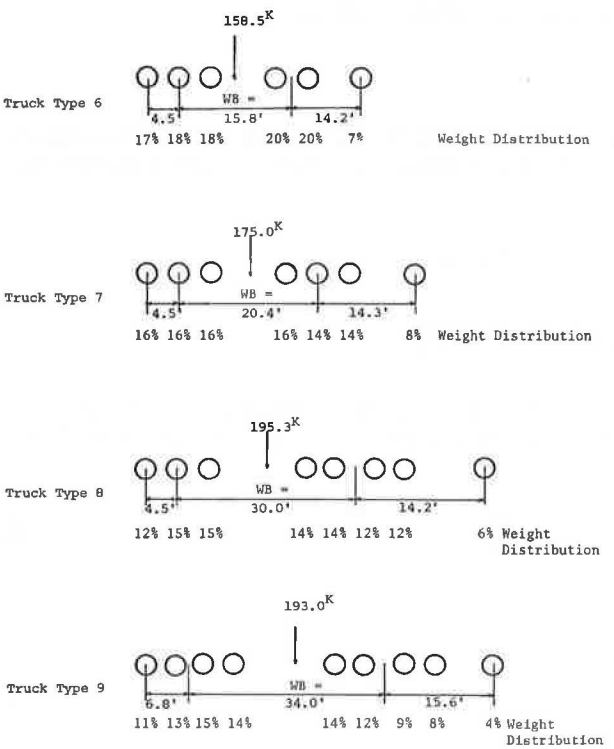

Figure 3. Typical trucks: types 10, 11, 12, and 15.

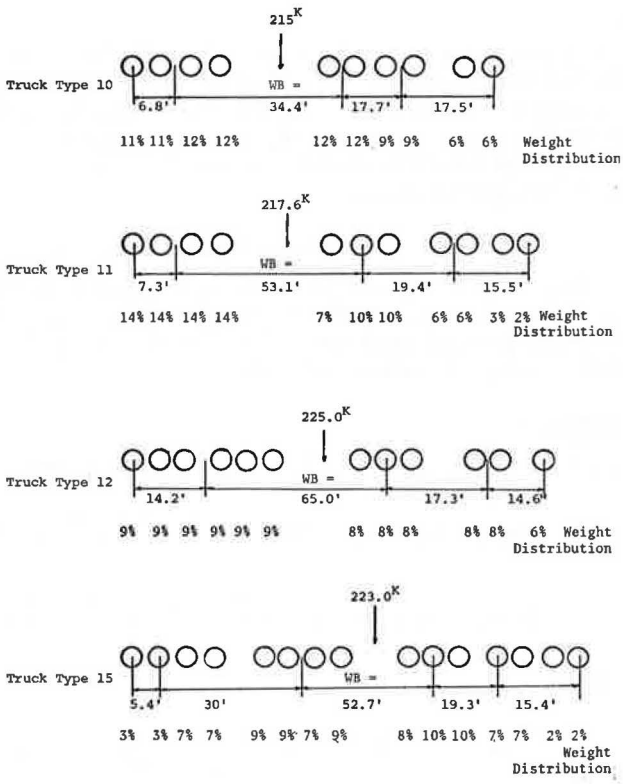

Figure 4. M_{PV}/GW versus span length: truck type 7.

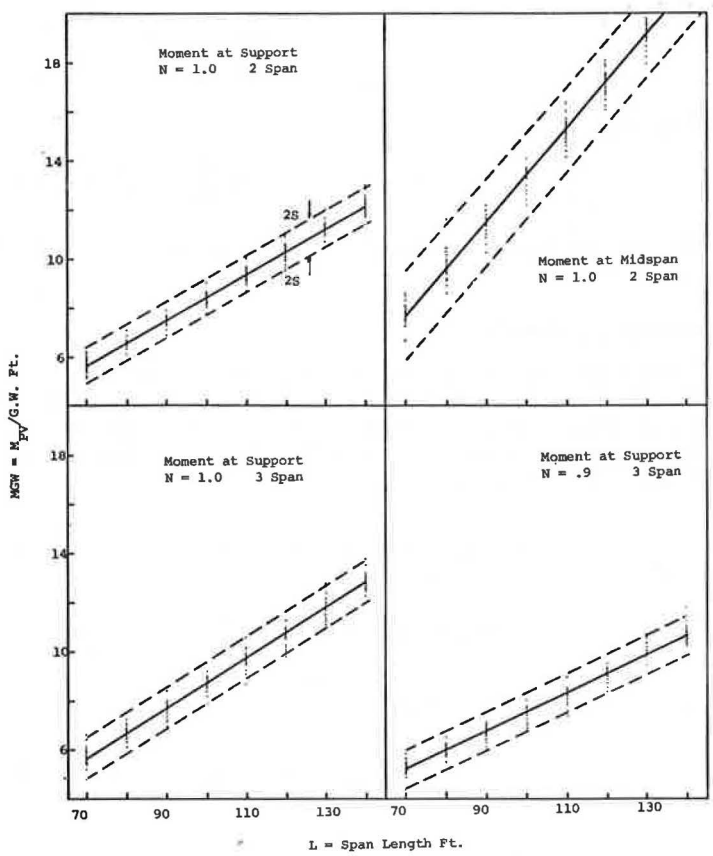

Equation 5 describes the difference in the induced girder moments caused by a permit vehicle and the design loading. Factor R thus can provide a gauge of the safety of the bridge, once the limiting value of R is established. R will be plotted as a function of span length L for the corresponding truck type of gross weights and moment locations. The induced AASHO moment may be governed by lane loading, and this was duly considered in computing M_{AASHO}.

ALLOWABLE RATIO R

The limiting value of R, designated as R_{out}, depends on the initial cross section of the girders and on the permissible increase in stress (allowed by the AASHO code) that is caused by unusual vehicles. The allowable R will be regulated by the type of bridge construction, i.e., shored or unshored.

Shored Construction

By using the basic equation f = M/S, the allowable stress equation is

$$\text{Design stress (AASHO) } f = \frac{M_{DL} + M_A (1.0 + I)}{S} = 0.55\ Fy \tag{7}$$

$$\text{Permit load stress } f = \frac{M_{DL} + M_{PV} (1.0 + 0.05)}{S} = 0.75\ Fy \tag{8}$$

Equating Eqs. 7 and 8 gives

$$\frac{M_{PV}}{M_A} = 0.345 \frac{M_{DL}}{M_A} + 1.295\ (1.0 + I)$$

However,

$$\frac{M_{PV}}{M_A} = R_{out}$$

Therefore,

$$R_{out_{shored}} = 0.345 \frac{M_{DL}}{M_A} + 1.295\ (1.0 + I) \tag{9}$$

For any bridge structure, R_{out} may be calculated by substituting M_{DL}, M_A, and I into Eq. 9.

Unshored Construction

Equations 7 and 8 must reflect section properties S_1 and S_2, noncomposite and composite section moduli respectively, to account for unshored construction. In unshored construction, dead-load stresses are calculated with noncomposite section modulus S_1 and live-load stresses are calculated with composite section modulus S_2. The induced stresses are as follows:

$$\text{Design stress (AASHO) } f = \frac{M_{DL}}{S_1} + \frac{M_A(1.0 + I)}{S_2} = 0.55\ Fy \tag{10}$$

$$\text{Permit load stress } f = \frac{M_{DL}}{S_1} + \frac{M_{PV}(1.0 + 0.05)}{S_2} = 0.75\ Fy \tag{11}$$

Equating Eqs. 10 and 11 gives

$$R_{out_{unshored}} = 0.345 \frac{S_2}{S_1} \frac{M_{DL}}{M_A} + 1.295\ (1.0 + I) \tag{12}$$

Although a majority of bridges are unshored, $R_{out_{shored}}$ is used in the development of the charts because it is always conservative. However, the more liberal $R_{out_{unshored}}$ (Eq. 12) may be used if the section properties S_1 and S_2 are known.

The dead-load moments for the bridges under study are based on estimations of dead-load weight per girder. These estimates were obtained from design curves developed by FHWA, which helped establish conservative values of girder weight. Examination of bridge plans (4) revealed that an 8½-in. slab at 120 lb/ft^3 gave a conservative approximation for slab and wearing surface. The estimated dead load/ft^2 for the various spans is given by Forbes and Heins (1). Girder spacing of 6.5 ft was used in estimating the M_{DL} for the curves because it yields minimum R_{out} values.

EXACT VALUE OF R

An estimate of M_{DL} (exact dead-load moment) is required to determine R_{out} for Eq. 9. A more rigorous equation has been developed that will account for deviation in dead-load moment estimations. Note that Eq. 9 is only for M_{DL} inasmuch as it is assumed that the term $[M_A (1.0 + I) + M_{DL}]$ always equals $(0.55\ Fy \times S)$. According to Eq. 9, when M_{DL} is overestimated, R_{out} increases and when M_{DL} is underestimated, R_{out} decreases because the equation requires the total moment to be equal to the design moment of $(0.55\ Fy \times S)$.

By assuming that a nondimensional quantity δ represents the percentage of deviation of the total actual moment from the design moment of magnitude $(0.55\ Fy \times S)$, Eq. 9 becomes

$$\frac{M_{DL} + M_A (1.0 + I)}{0.55 + \delta} = \frac{M_{DL} + M_{PV} (1.0 + 0.05)}{0.75}$$

or

$$R_{out} = \frac{M_{PV}}{M_A} = \frac{(0.345 - 1.74\ \delta)}{(1.0 + 1.82\ \delta)} \frac{M_{DL}}{M_A} + \frac{1.295\ (1.0 + I)}{(1.0 + 1.82\ \delta)} \tag{13}$$

However,

$$M_{PV} = \frac{(0.75\ Fy \times S - M_{DL})}{(1.0 + 0.05)}$$

Therefore Eq. 12 gives the value of δ as

$$\delta = \frac{M_{DL} + M_A (1.0 + I)}{Fy \times S} - 0.55 \tag{14}$$

A pictorial representation of Eq. 12 is shown in Figure 5. When δ is zero (Fig. 5), the total moment $[M_A (1.0 + I) + M_{DL}]$ equals the design moment at a magnitude of $(0.55\ Fy \times S)$, and R_{out} is known exactly. When M_{DL} is overestimated, δ is positive and R_{out} decreases. If M_{DL} is underestimated, δ is negative and R_{out} increases.

When analyzing a particular bridge with known properties, Eq. 12 may be used. Equation 12 can also be used when the bridge is overdesigned. The difference between the design moment $(0.55\ Fy \times S)$ and the known existing moment equals $-\delta$, and, when substituted in Eq. 12, it will produce a larger R_{out} ratio. Thus, a heavier vehicle would be permitted to cross the bridge.

CHARTS

Equation 6 has been plotted as a function of span length, gross weight, and type of structure (1). Some of these charts for truck type 7 are shown in Figures 6 through 10. The limiting value of R (R_{out}, Eq. 8) is plotted on each of these figures.

The only parameters that are required for using these charts are the permit vehicle type [classified by number of axles (Figs. 1 through 3)], gross weight, type of bridge, and span length.

Figure 5. Allowable moment criteria.

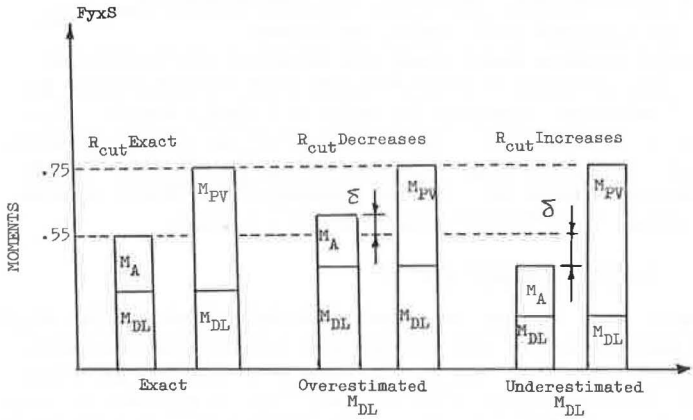

Figure 6. R versus GW: truck type 7.

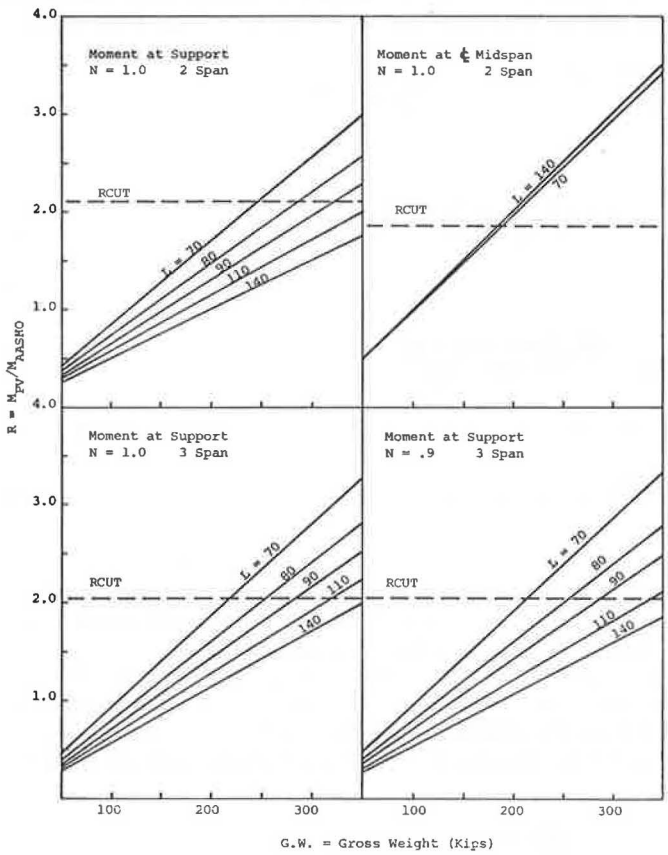

Figure 7. R versus GW: truck type 7.

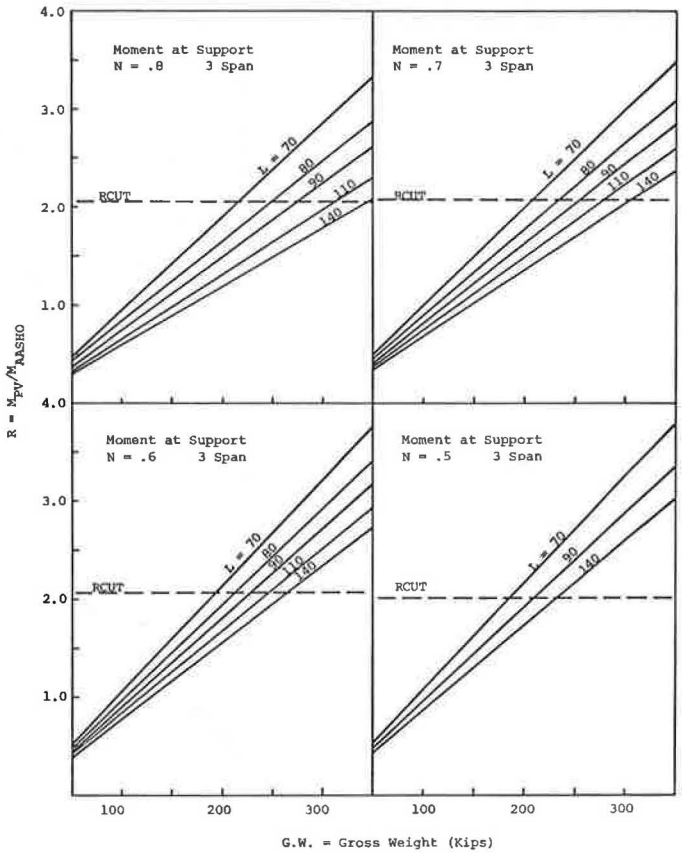

Figure 8. R versus GW: truck type 7.

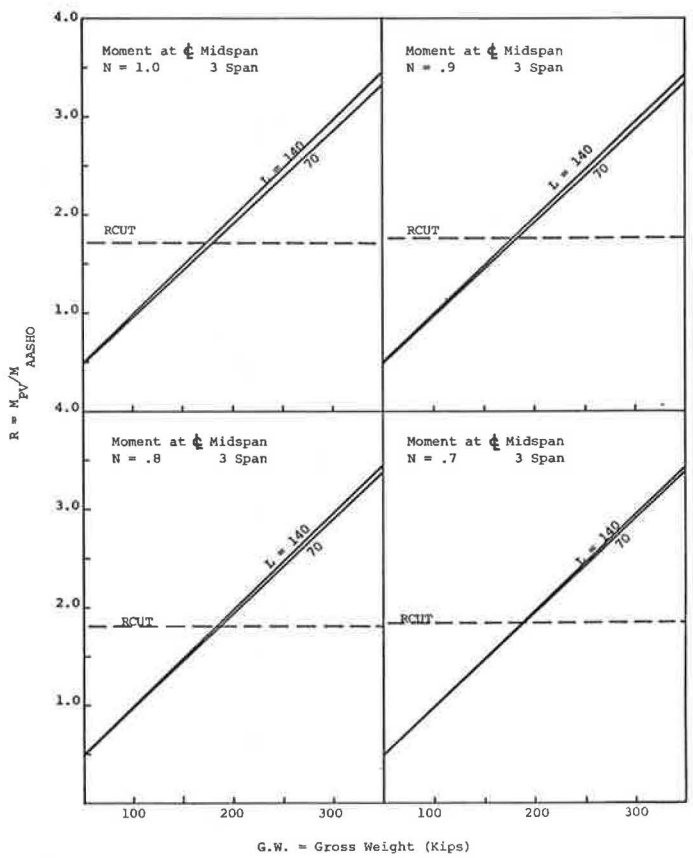

Figure 9. R versus GW: truck type 7.

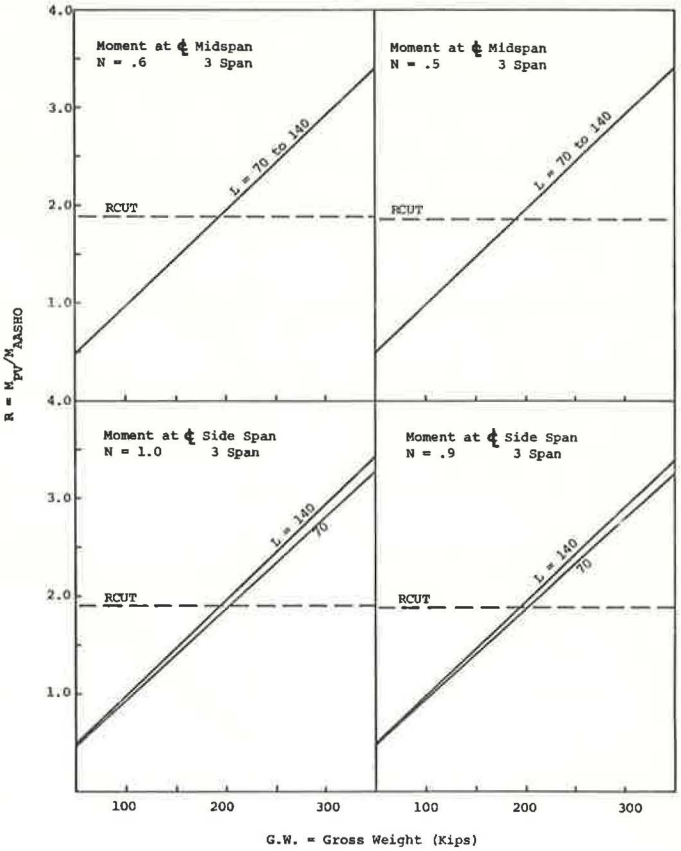

Figure 10. R versus GW: truck type 7.

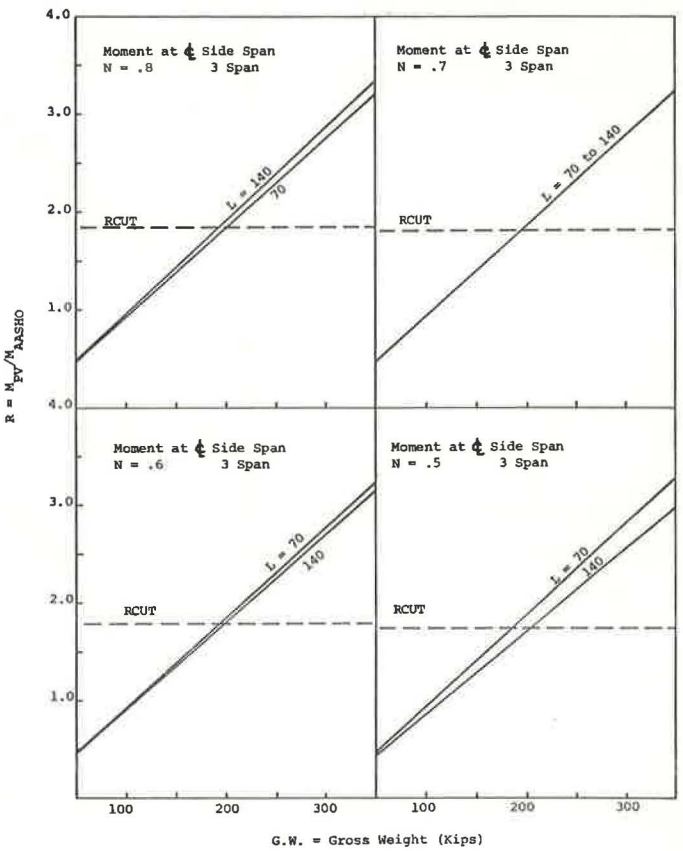

Figure 11. Three-span girder details.

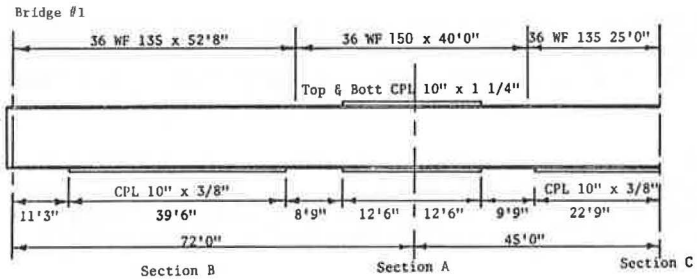

Figure 12. Permit vehicle characteristics.

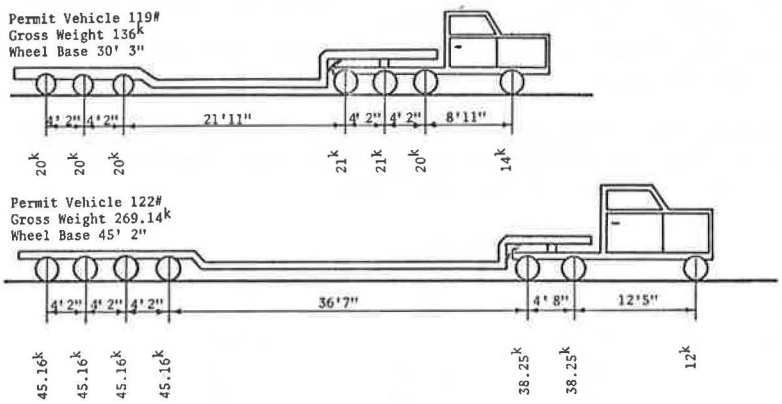

Table 1. Section properties and moments.

Section	Type	Section Modulus (NC)[a] Top ($in.^3$), Steel Flange	Section Modulus (NC)[a] Bottom ($in.^3$), Steel Flange	Section Modulus (C)[b] Top ($in.^3$) Steel Flange	Section Modulus (C)[b] Top ($in.^3$) Concrete Slab	Section Modulus (C)[b] Bottom ($in.^3$), Steel Flange	M_{DL} (kip-ft)	M_A (kip-ft)	M_{PV1} (kip-ft)	M_{PV2} (kip-ft)
A	NC	849.0	849.0	849.0	—	849.0	-690.9	-635.0	-501.0	-1,000.0
B	C	454.0	530.0	357.0	16,700.0	739.0	371.0	690.0	624.0	1,220.0
C	C	454.0	530.0	357.0	16,700.0	739.0	361.0	716.0	683.0	1,352.0

[a]NC = noncomposite. [b]C = composite.

Table 2. Stresses.

Section	Dead-Load Stress[a] Top, Steel Flange	Dead-Load Stress[a] Bottom, Steel Flange	Live-Load Stress[a] for AASHO Top Steel Flange	Live-Load Stress[a] for AASHO Top Concrete Slab	Live-Load Stress[a] for AASHO Bottom, Steel Flange	Live-Load Stress[a] for PV1 Top Steel Flange	Live-Load Stress[a] for PV1 Top Concrete Slab	Live-Load Stress[a] for PV1 Bottom, Steel Flange	Live-Load Stress[a] for PV2 Top Steel Flange	Live-Load Stress[a] for PV2 Top Concrete Slab	Live-Load Stress[a] for PV2 Bottom, Steel Flange
A	+9.76	-9.76	+9.0	—	-9.0	+7.08	—	-7.08	+14.12	—	-14.12
B	-9.80	+8.40	-2.35	-0.414	+11.37	-2.10	0.374	+10.15	-4.09	0.731	+19.78
C	-9.54	+8.18	-2.40	-0.429	+11.59	-2.29	0.409	+11.09	-4.55	0.810	+22.0

[a]Measured in ksi.

APPLICATION

Nine existing bridges were completely analyzed to show the reliability of the charts and their application in predicting induced maximum stresses caused by permit vehicles (1). Ratios of stresses obtained by an exact analysis were compared to the chart values. In all instances R_{out} values were always conservative and provided safe analysis by use of the charts.

Figure 11 shows the analysis of a three-span continuous bridge. The bridge was composite in the positive moment region; made of A36 steel; and had a 7-in. concrete slab, 2-in. wearing surface, 7-ft, 7-in. girder spacing, and a computed 1.038 kips/ft dead load per girder. The bridge was subjected to two different seven-axle (heavy) trucks, as shown in Figure 12.

The safety of the three-span structure after these trucks had passed over it can be seen in Figures 6 through 10. For an end span ratio of N = 72 ft/90 ft = 0.80 and with examination of $M_{support}$ (Fig. 7), M_{o1} at midspan (Fig. 8), and M_{o1} at side span (Fig. 10), for GW = 136 kips, and L = 90 ft, the R value is below the R_{out} at all moment locations. Therefore, permit vehicle 1 (PV1) may cross the bridge.

For the 269-kip permit vehicle (PV2), the R value for the moment at M_{o1} of midspan and end span exceed R_{out}; therefore, this truck would not be permitted to cross the bridge.

The exact stress analysis of this bridge based on AASHO and permit loads is summarized in Tables 1 and 2. The total dead-load and live-load governing stresses at the critical points (A, B, and C) on the girder are as follows:

	Stress (ksi)		
Loading	A	B	C
AASHO	±18.76	+19.77	+19.77
PV1	±23.88	+18.55	+19.27
PV2	±23.88	+28.18	+30.18

The allowable stress on the steel based on the overloads is 0.75 Fy = 27.0 ksi. PV1 does not cause an overstress at any sections; therefore, it may be issued a permit. PV2 does cause an overstress; thus no permit would be granted. This is the same conclusion that was reached when the charts were used. The concrete stress is less than 0.40 f_c' and does not govern.

CONCLUSIONS

A series of charts have been developed (1) that can be applied toward determining the safety of continuous span composite bridges that are subjected to heavy vehicle loads. These charts are easily used and are functions of vehicle gross weight, truck type based on the number of axles, span length, and location of the moment on the girder.

ACKNOWLEDGMENT

This research was sponsored by the Maryland State Roads Commission and the FHWA. Their suggestions, guidance, and encouragement are gratefully acknowledged.

REFERENCES

1. Forbes, R. C., and Heins, C. P. Analysis Charts for Use in Issuing Vehicle Permits. University of Maryland, Civil Engineering Rept. 49, June 1973.
2. Standard Specifications for Highway Bridges. AASHO, 1969.
3. Moments, Shears and Reactions for Continuous Highway Birdges. AISC, New York, 1966.
4. Bureau of Public Roads, U.S. Dept. of Commerce. Standard Plans for Highway Bridges. U.S. Govt. Printing Office, Washington, D.C., Vols. 1, 4, 1962.

COMPARISON OF MEASURED AND COMPUTED LOAD-DEFLECTION BEHAVIOR OF TWO HIGHWAY BRIDGES

Edwin G. Burdette and David W. Goodpasture, Department of Civil Engineering, University of Tennessee, Knoxville; and
Stephen K. Doyle, Tennessee Valley Authority

Four deck girder highway bridges in Tennessee, located in an area to be inundated as part of a Tennessee Valley Authority reservoir, were tested under static load to failure. Research was directed toward comparing actual bridge behavior with that which could be calculated by using accepted structural analysis methods. This paper is concerned specifically with a comparison of measured and computed load-deflection relationships of two steel girder continuous bridges. Load-deflection curves calculated on the basis of strain compatibility relationships, assuming that the entire bridge with curbs acts as a wide beam, gave results that compared reasonably well with the actual load-deflection curves. Actual and calculated curves were particularly close for bridge A. The behavior of bridge B in the elastic region indicated that, although no provision was made to ensure composite action, such action did exist. The computed load-deflection curve compared very well with the measured curve in the elastic range when composite action was assumed to exist. It was concluded that the method presented for the prediction of load-deflection relationships was satisfactory. The total moment capacities calculated by this method were close to the measured capacities for both bridges.

•FOUR highway bridges, located in Franklin County, Tennessee, were tested to failure during the summer of 1970. These bridges were located in an area that has since been flooded as a part of the Tennessee Valley Authority's Tims Ford Reservoir. At the time of testing, these bridges had already been replaced by newer bridges at higher elevations.

Each of the two bridges considered was a two-lane, continuous deck girder bridge, whose girders consisted of steel rolled beams with cover plates at interior supports. Bridge A was a four-span continuous bridge with span lengths of 70, 90, and 70 ft. It was designed in 1963 for an HS 20 loading. Studs were provided in the positive moment regions to ensure composite action.

Bridge B had three spans with span lengths of 45, 60, and 45 ft. It was designed in 1956 for an H-15 loading. No provision was made for composite action.

Both bridges were excellent test specimens. Bridge A was on a slight sag vertical curve; each was straight and had a 90-deg skew. Figures 1 and 2 show photographs of the two bridges.

The testing procedure is described in detail elsewhere (1, 2, 3). The position of the applied loads is shown in Figure 3. The loads on bridge A are intended to simulate two HS trucks, one in each traffic lane. Because of difficulties in rock drilling, only six loading points were used on bridge B.

Among other data obtained from the tests were load-deflection curves for various points on the bridge decks. An average of the deflection readings over the four girders at the centerline of the loaded span was obtained so that a representative load-deflection curve for each bridge could be plotted. These curves will be compared to the load-

Publication of this paper sponsored by Committee on Dynamics and Field Testing of Bridges.

Figure 1. Bridge A.

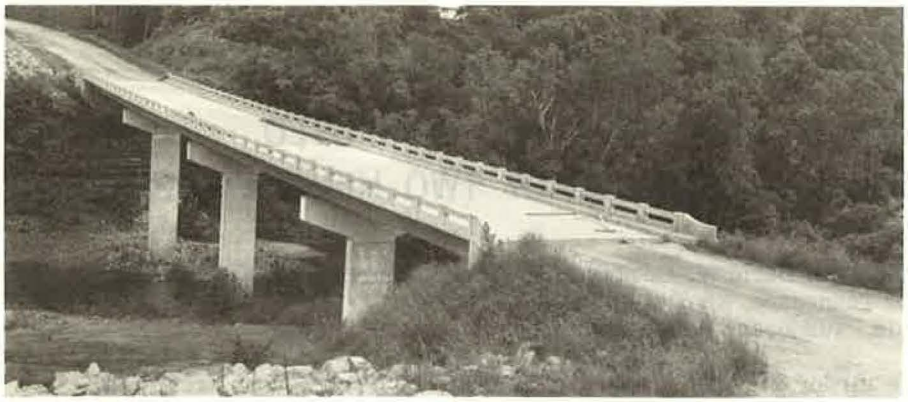

Figure 2. Bridge B.

Figure 3. Position of loads used for bridges A and B.

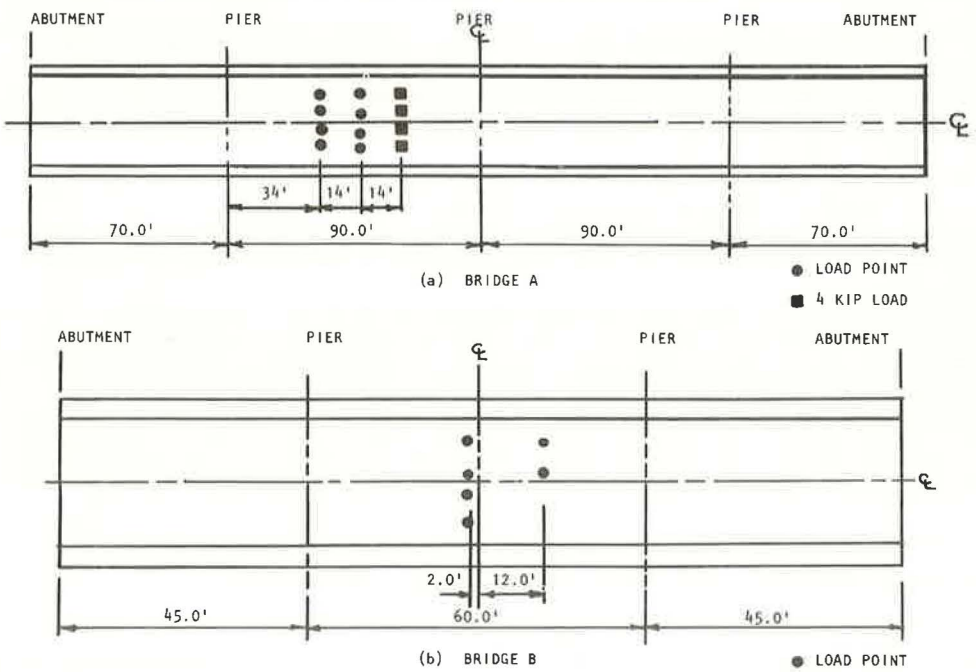

deflection curves obtained analytically. Figures 4 and 5 show photographs of the bridges at failure.

A comparison of measured and computed ultimate strengths of the four bridges was discussed by Burdette and Goodpasture (2). This paper compares the measured load-deflection relationships for the two steel girder continuous bridges with results of an analytical solution based on strain compatibility relationships.

METHOD FOR OBTAINING THEORETICAL LOAD-DEFLECTION CURVES

The method used for calculating deflections for particular loads on the two bridges was based on the determination of moment-curvature relationships (4, 5). Load-deflection curves were determined by taking a typical cross section of the bridge and developing a resisting moment versus curvature relationship or M-ϕ curve. The curvature, ϕ, is equivalent to M/EI for an elastic member. The deflections for these bridges were determined with the ICES STRUDL-II computer program and the principle of superposition. The basic idea in this procedure is that, as load on a bridge increases beyond first yielding, the bridge properties change. To obtain the total deflection of the bridge requires that the deflections be added or be superimposed every time the properties of the bridge change. So that these procedures could be used several assumptions were made.

Assumptions

The locations of sections at which plastic hinges would form were predicted. For bridge A, these were at the line of applied loads nearest midspan and at the section over the pier nearest the first section. For bridge B, plastic hinges were assumed to form at the line of applied loads nearest midspan and over the two piers. The actual test confirmed these assumptions except that plastic hinges formed at the ends of the cover plates a short distance from the piers—on the other side of the piers from where the loads were applied rather than directly over the piers.

The bridges were idealized to facilitate computations. Curvature caused by the crown in the roadway and other shapes such as chamfered edges on the cross sections were idealized or ignored. Any effect of handrails was not considered. Supports were taken to be at the centerline of bearing and assumed to act as knife edges. Reinforcing steel in the bridge decks was not considered. The load caused by the hydraulic rams was assumed, for calculation purposes, to have uniform lateral distribution; that is, the loads were treated as line loads extending across the bridge deck.

The bridges were considered to act as single beams. Bending about the longitudinal axis or the axis along the roadway centerline was not considered. Calculations considered the curbs or raised sidewalk portions as integral parts of the bridges. No effort was made in these computations to investigate individual parts of the bridge, i.e., comparing the amount of load carried by an interior girder versus that carried by an exterior girder.

Material Properties

Stress-Strain Curves for Concrete—With the values of f_c' determined from the compression tests and formulas (6), idealized stress-strain curves for concrete were developed for each bridge. Taking $0.85 \times f_c'$ as the maximum flexural stress the concrete can attain and $w^{1.5}(33)f_c'$ as the modulus of elasticity of concrete, where w is the weight of concrete in pounds per cubic foot, enabled a stress-strain curve for the concrete in each bridge to be developed. Three assumptions were made so that the curves could be drawn: (a) all concrete weighed 145 lb/ft^3, (b) the stress was constant after reaching a maximum of $0.85\ f_c'$ and up to a strain of 0.002, and (c) the modulus of elasticity was constant up to a stress value of $0.85\ f_c'$. No attempt was made to develop the curves past a strain of 0.002. The assumptions given (6) were used to calculate moment and curvature at concrete strains greater than 0.002. Figure 6 shows the stress-strain curves for the concrete in the two bridges.

Stress-Strain Curves for Steel—The stress-strain relationships for the steel in each bridge, which are shown in Figure 6, were used in the computations.

Figure 4. Bridge A at failure.

Figure 5. Bridge B at failure.

Figure 6. Stress-strain curves.

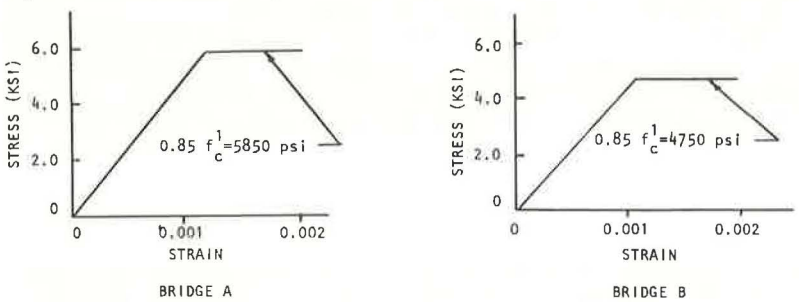

(a) STRESS-STRAIN CURVES IN FLEXURE FOR CONCRETE IN BRIDGE DECKS

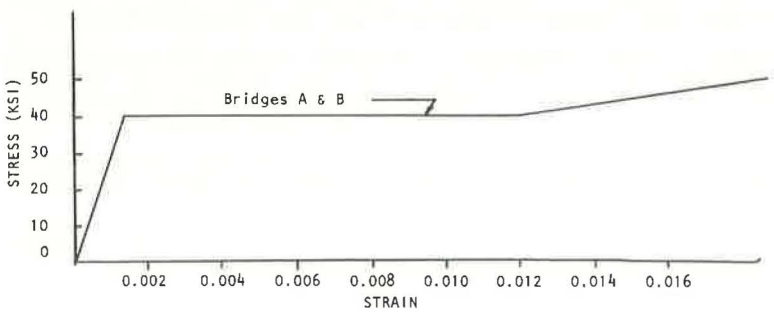

(b) STRESS-STRAIN CURVE FOR STEEL IN BRIDGES A AND B

Determination of M-ϕ Curves

The determination of the M-ϕ relationships for the positive bending moment region of bridge A involved consideration of both the concrete and the steel, whereas the M-ϕ curves for bridge B and for the negative bending region over the piers of bridge A considered only the steel girders. In the regions where only steel was considered, the M-ϕ curves were calculated by assuming noncomposite behavior because there were no shear studs between the steel beams and the concrete deck. The methods used to calculate M-ϕ curves required application of the following necessary relationships:

1. Equilibrium of horizontal forces and moments,
2. Assumption of linear strain distribution,
3. Knowledge of the stress-strain relationships for concrete and steel, and
4. Perfect bond between beams and bridge deck where composite construction was assumed.

Idealized M-ϕ diagrams for the negative moment region of bridge A and for both positive and negative moment regions of bridge B were obtained quite simply. First, the moment and curvature at first yield of the steel were calculated on the basis of elastic theory, and this point was plotted. Then, the plastic moment of the cross section was calculated, and a horizontal line representing this moment was plotted on the M-ϕ diagram. Finally, a straight line intersecting the horizontal line representing the plastic moment was drawn from the origin ($M = 0$, $\phi = 0$) through the point at yield. The resulting M-ϕ diagrams for positive and negative moment regions of bridge B are shown in Figure 7.

The M-ϕ curve for the positive moment region of bridge A could not be so easily idealized. The method used to calculate points on the curve is essentially that described by Warwaruk, Sozen, and Siess (4) and Khachaturian and Gurfinkel (5). The diagram was assumed to be perfectly linear up to first yield of the steel. From that point forward, points on the curve were calculated on the basis of a chosen strain in the extreme compressive fibers of the concrete. The M-ϕ diagrams for both positive and negative moment regions of bridge A are shown in Figure 8.

Load-Deflection Curves

The load-deflection curves for bridges A and B were developed by using the STRUDL-II subset of the ICES computer program, the law of superposition, and the M-ϕ curves developed previously.

Method of Computation—The plane frame option of the STRUDL-II subset of the ICES program uses a stiffness method of analysis to calculate moments, shears, reactions, and deflections of a beam or frame subjected to a prescribed loading. This program requires that the moments of inertia and modulus of elasticity be specified constants for each member. If a beam is not of uniform cross section throughout its length, a joint can be chosen at each section where the beam cross section changes, and appropriate E and I values can be specified for the several beams needed to represent the actual beam being analyzed. This procedure was used to analyze bridges A and B with cross-section properties that were not constant throughout their length.

Both bridges were treated as wide continuous beams as was done in the determination of M-ϕ curves. The beams were subjected to concentrated loads so that maximum moment at the load nearest midspan was produced. The loading was increased until enough plastic hinges were formed to create a mechanism, and the total load required to form the mechanism was considered to be the ultimate load for the bridge.

When the ultimate moment was reached at a section with an M-ϕ curve like those for bridge B and the negative moment region of bridge A, the structure was modified for further load application by considering that a hinge existed at the section. The load, acting on the "new" structure with a hinge, was increased until ultimate moment was reached at another section. If this section also had an M-ϕ relationship like those noted, a second hinge was introduced in the structure with the result that a third structure was formed. The load acting on this structure was increased until another plastic hinge was formed. This procedure was continued until a mechanism existed, and the

Figure 7. Moment-curvature curves for bridge B.

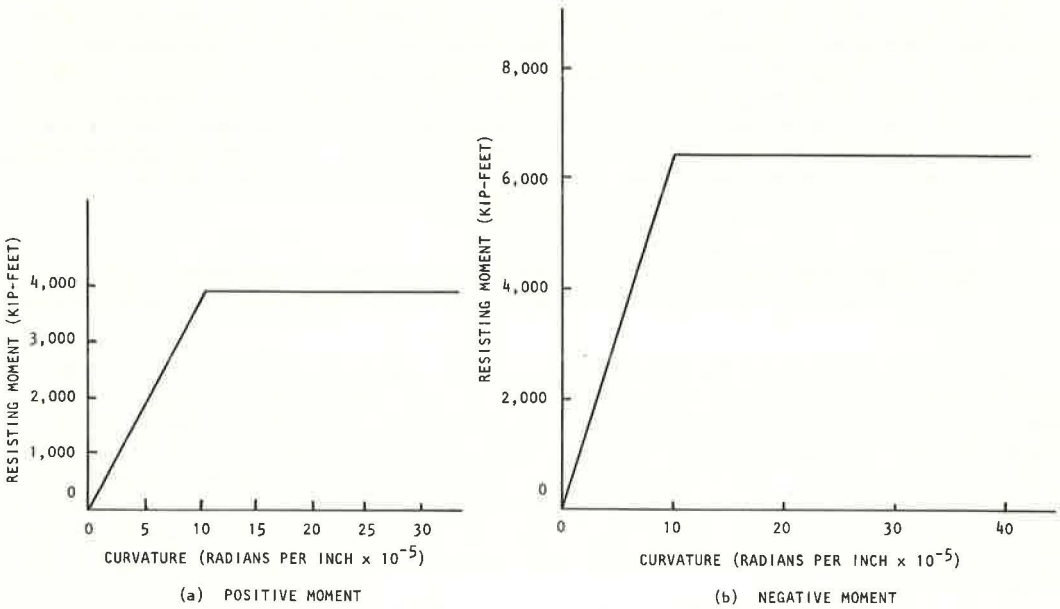

Figure 8. Moment-curvature curves for bridge A.

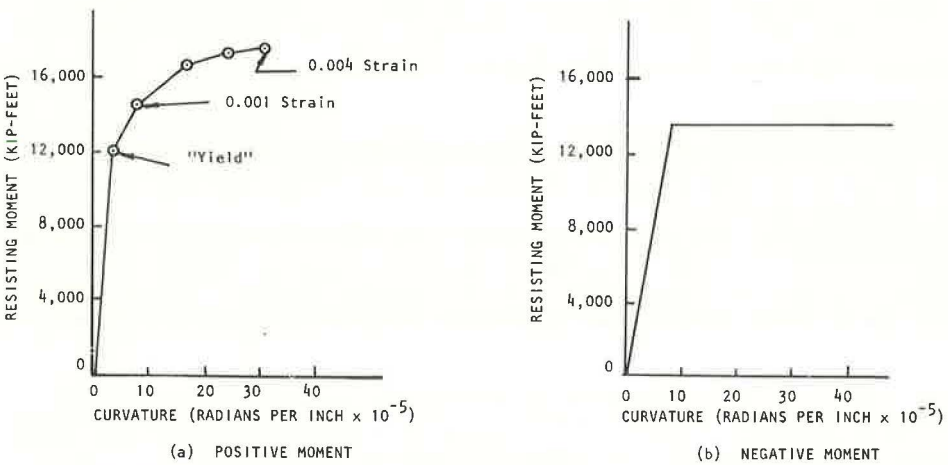

ultimate load was calculated as the sum of the loads that were acting on the structure at various stages to form plastic hinges.

If the M-ϕ curve for the section of maximum moment was like that for the positive moment region of bridge A, the fact that the section does not reach ultimate moment immediately after stopping to be elastic necessitates a somewhat modified approach. The procedure for handling this case was as follows:

1. When the load was sufficient to cause a moment at the section equal to that at which the section no longer behaved elastically, a new structure was considered for further application of load.
2. This new structure for additional load could not be considered as having a hinge at the maximum moment section, because the M-ϕ curve still had a positive slope. Instead, a small length of structure centered at this section was modified to have an EI consistent with the slope of the M-ϕ curve beyond the point of first loss of elastic action.
3. The length of this revised section was taken as the overall depth of the member which, for the composite section of bridge A, was approximately 4 ft.

One further consideration was required for bridge A. No provision was made for a downward reaction at the abutments; thus, during the test, the bridge lifted off the abutment nearest the loaded span. This occurrence was considered in the analysis by making appropriate modification to the structure at the load that caused a zero reaction at the abutment.

Results—The calculated load-deflection curves for the two bridges are shown in Figures 9 and 10 with the average curve obtained experimentally.

COMPARISON OF RESULTS

The calculated and measured load-deflection curves for bridge A compared remarkably well, as shown in Figure 9. The computed ultimate load was 1,270 kips, and the measured ultimate load was 1,250 kips.

The two curves shown in Figure 10 for bridge B do not compare so favorably. There are two probable reasons for this lack of agreement: (a) The loading on the bridge was not perfectly symmetrical (Fig. 3), and (b) the calculated behavior of the bridge was based on noncomposite behavior, whereas the actual behavior as indicated by strain measurements reflected a high degree of composite action up to near yielding of the steel. The first reason probably explains why the actual ultimate load (640 kips) was less than the computed ultimate (696 kips); that is, not all girders reached their plastic moment capacity under the same loading.

The second reason, i.e., the assumption of composite behavior, explains the discrepancy between the two curves for bridge B in the elastic region. The line obtained on the basis of full composite action coincided almost identically with the measured curve in the elastic range (Fig. 10).

CONCLUSIONS

The method used in this paper to predict load-deflection relationships for the two bridges proved to be satisfactory. [A detailed discussion of the research results (1) and of certain aspects of the research (2, 3) is available.] The ultimate load, calculated on the basis of considering the bridge to act as a single wide beam, compared closely with that obtained in the field tests. This suggests the possibility of basing ultimate strength design methods on a comparison between the total bridge moment and the sum of the ultimate moment capacities of the individual girders.

That composite action existed in bridge B, even though it had been subjected to severe overloads and to vibratory loads before static tests began, is of interest. This indicates that composite action will generally occur in a deck girder bridge up to loads well beyond the design load for the bridge. Laboratory tests to confirm this observation and, thus, to lead to design criteria that appropriately reflect this phenomenon would appear to be in order.

Figure 9. Comparison of measured and computed load-deflection curves for bridge A.

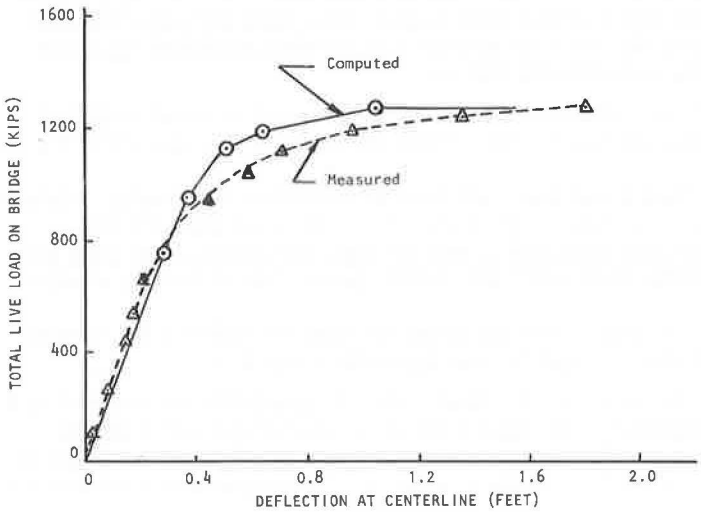

Figure 10. Comparison of measured and computed load-deflection curves for bridge B.

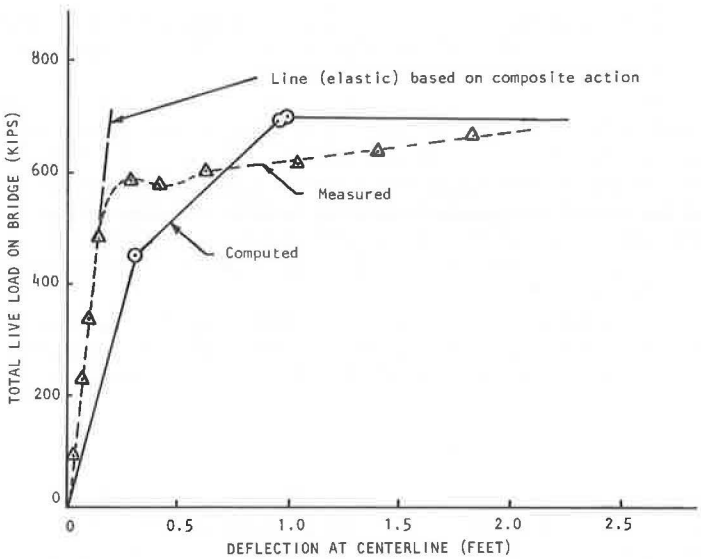

ACKNOWLEDGMENT

This project was performed as a part of a research contract between the Civil Engineering Department, University of Tennessee, and the Bureau of Highways, Tennessee Department of Transportation, in cooperation with the Federal Highway Administration. The opinions, findings, and conclusions expressed are those of the authors and not necessarily those of the State of Tennessee or the Federal Highway Administration.

REFERENCES

1. Burdette, E. G., and Goodpasture, D. W. Full-Scale Testing. Tennessee Department of Transportation and Federal Highway Administration, Final rept., Dec. 31, 1971.
2. Burdette, E. G., and Goodpasture, D. W. Comparison of Measured and Computed Strengths of Four Highway Bridges. Highway Research Record 382, 1972, pp. 38-50.
3. Burdette, E. G., and Goodpasture, D. W. Tests of Four Highway Bridges to Failure. Jour. Structural Division, Proc. ASCE, March 1973.
4. Warwaruk, J., Sozen, M. A., and Siess, C. P. Investigation of Prestressed Reinforced Concrete for Highway Bridges—Part III: Strength and Behavior in Flexure of Prestressed Concrete Beams. University of Illinois Engineering Experiment Station Bull. 464, Urbana, 1962.
5. Khachaturian, N., and Gurfinkel, G. Prestressed Concrete. McGraw-Hill, 1969.
6. Building Code Requirements for Reinforced Concrete. American Concrete Institute (ACI 318-71), 1971.

ASSESSMENT OF FATIGUE LIFE OF A STEEL GIRDER BRIDGE IN SERVICE

Fernando Cicci, De Havilland Aircraft of Canada, Ltd.; and
Paul Csagoly, Ministry of Transportation and Communications, Ontario

To assess the fatigue life of welded, cover-plated steel girders, strain gauges were placed in critical locations on the superstructure of the Leslie Street overpass on the Toronto Bypass. Data were gathered for 200 hours in 12-hour continuous tape recording sessions. Analysis of the data revealed that normal traffic caused a live-load stress peak of 4,000 psi (2757 MPa) only once in 10 hours, which is less than 50 percent design live-load stress. Stress data gathered by various agencies during the past few years seem to indicate that either design stress does not occur at all or it occurs with such a low frequency that the development of any fatigue situation is precluded. The phenomenon is associated with the low probability of the simultaneous, multiple presence of loaded commercial vehicles on a structure. The problem is therefore statistical in nature. Its recognition appears to be in conflict with the prevailing concept used in fatigue consideration of highway bridges.

•STRUCTURAL engineers in the Ministry of Transportation and Communications, Ontario, expressed considerable concern when an internal, cover-plated steel beam failed in the Yellow Mill Pond Viaduct on I-95, Bridgeport, Connecticut, in 1970. The failure originated in a crack at the toe of the fillet weld that spread along the end of the cover plate and through the flange. It had extended 16 in. (406 mm) up into the web before it was detected. Subsequent inspection revealed the presence of numerous smaller cracks at the cover plate ends at several locations in the bridge.

The ministry has a number of bridges under its jurisdication similar in construction to and built about the same time (1958) as the Yellow Mill Pond Viaduct. One of them, the Leslie Street overpass, is located on the Toronto Bypass.

The Toronto Bypass is a 12-lane artery (three core and three collector lanes in both directions) which carries 146,000 ADT (at Leslie Street), of which an estimated 13.5 percent is commercial. These figures are comparable to those obtained at the Yellow Mill Pond Viaduct (7).

The Ontario Highway Traffic Act, which controls heavy commercial vehicles in the province, permits gross vehicle weights far in excess of those in Connecticut. Five-axle tractor and semi-trailer (3S-2) combinations can carry 84,000 lb (38 000 kg) if they are conventionally constructed and 93,000 lb (42 000 kg) if they are designed in accordance with the provisions of the Ontario bridge formula (1971). In addition, eight-axle vehicle trains and five-axle special permit vehicles (usually floats transporting construction equipment) can have as much as 140,000 lb (64 000 kg) gross weight. The comparable maximum vehicle weight in Connecticut is 73,000 lb (33 000 kg).

The core section of the Leslie Street overpass consists of six simply supported spans of various lengths. The cover plates are fastened to the flanges by intermittent welds of questionable quality, which would make this structure most susceptible to fatigue cracking. [A 5,000-psi (34.47 MPa) limit for allowable range of stress F_{sr} over 2,000,000 cycles is suggested (6).] The purpose of the investigation was to establish stress-range frequencies at various points of the superstructure and to predict expected service life of the bridge with available laboratory test data.

Publication of this paper sponsored by Committee on Dynamics and Field Testing of Bridges.

Figure 1. Schematic of test site.

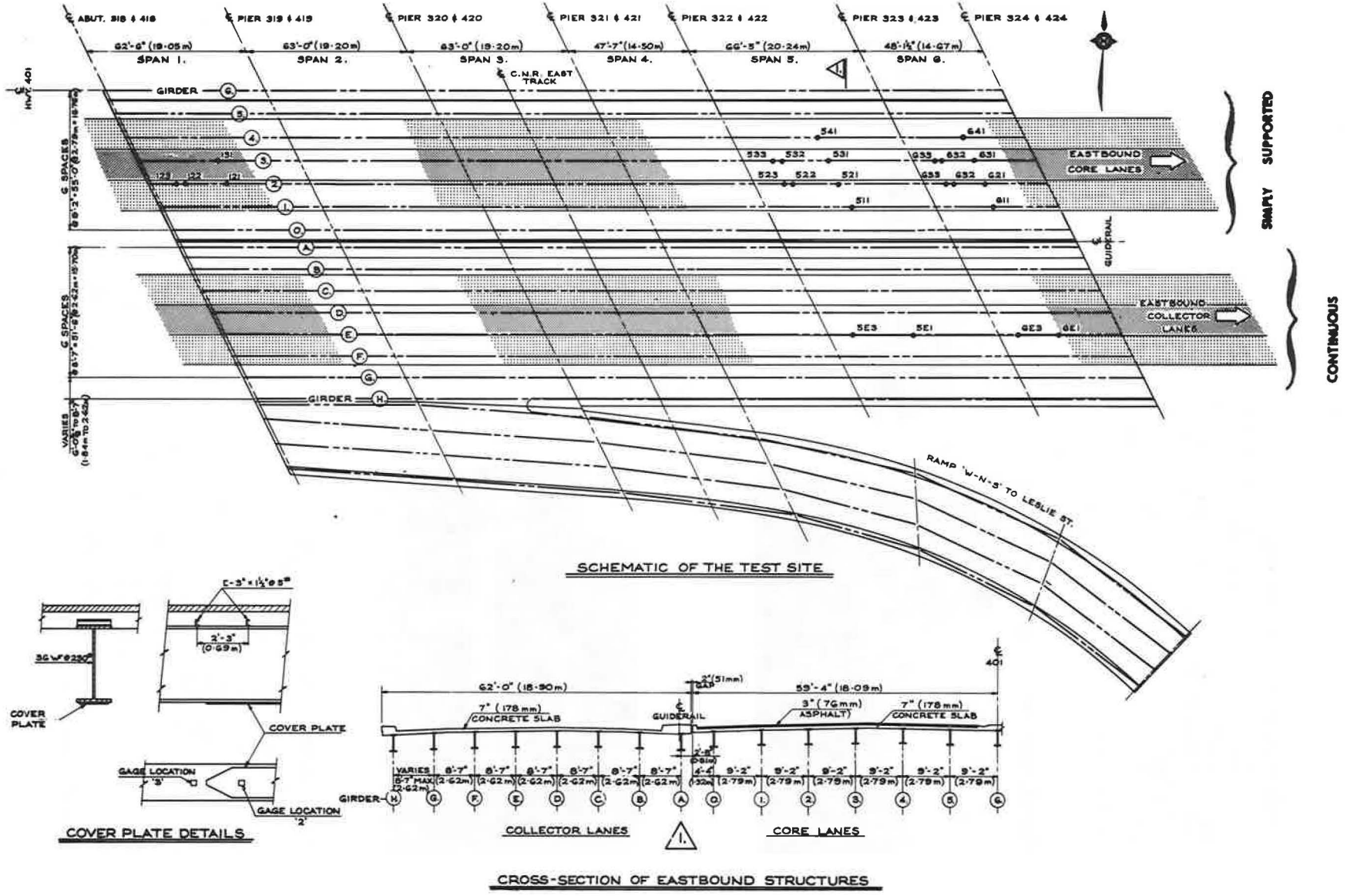

Table 1. Girder and cover plate geometry.

Span Number	Bearing, Center-to-Center Distance (ft)	Beam Size	Cover Plate		
			Length (ft)	Width (in.)	Thickness (in.)
1, 2, 3	62.0	36WF230	27.5	14.0	0.375
4, 6	46.6	36WF150	14.5	10.0	0.375
5	65.5	36WF230	34.5	14.0	0.625

Note: 1 in. = 25.4 mm; 1 ft = 0.3048 066 m.

Figure 2. Welding details on Leslie Street overpass.

Figure 3. Load-testing vehicle.

Figure 4. Deflectometer.

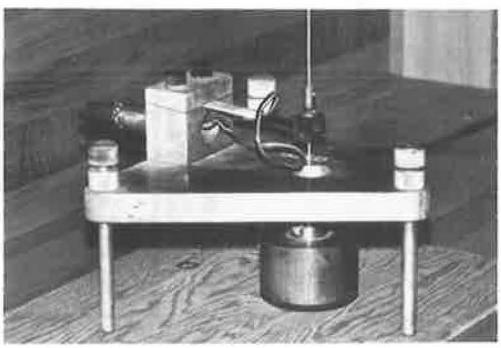

Table 2. Placement of deflectometers (phase 1).

Station	Span	Beam	Position on Beam
1	5	11	East end of cover plate
2	5	11	Midspan
3	5	11	West end of cover plate
4	5	3	Midspan
5	5	2	Midspan
6	6	3	Midspan
7	—	—	—
8	6	1	East end of cover plate
9	6	1	West end of cover plate
10	5	1	East end of cover plate
11	5	1	West end of cover plate

Table 3. Deflections during test vehicle runs.

Run	Deflection (in.) at Station										
	1	2	3	4	5	6	7	8	9	10	11
1	0.10	0.08	0.08	—	—	—	—	—	—	—	—
2	0.24	0.23	0.20	—	—	—	—	—	—	—	—
3	0.20	0.19	0.17	—	—	—	—	—	—	—	—
4	—	—	—	0.17	0.30	0.07	—	0.12	0.16	0.22	0.29
5	—	—	—	0.33	0.31	0.18	—	0.06	0.06	0.11	0.13
6	—	—	—	0.21	0.13	0.08	—	—	—	0.06	0.07
7	—	—	—	0.12	0.24	0.08	—	0.11	0.14	0.16	0.22
8	—	—	—	0.23	0.21	0.17	—	0.04	0.04	0.08	0.08
9	—	—	—	0.13	0.06	0.08	—	—	—	0.02	0.02

Note: 1 in. = 25.4 mm.

This report describes the equipment used to acquire data and the methods of reducing the data to produce the required frequency distribution. An attempt has been made to apply Miner's hypothesis to predict the service life of the bridge.

TEST SITE

The skewed bridge decks that were of interest in this test program are at the western end of the Leslie Street overpass. Figure 1 shows the six core lanes and the three eastbound collector lanes.

In the core area, which was built in 1958, each span of the structure is simply supported with the beam ends resting on neoprene bearings. There are six spans including number 1 at the extreme western end. There are three different span lengths and various girder sizes and bottom flange cover plate geometries. The combinations are given in Table 1.

Across the width of the core area there are 13 girders measuring 9 ft, 2 in. (2.79 m) from center to center. For this test program, the girders were designated 0, 1, 2, . . . , 10, 11, and 0^1 from south to north. The 0 and 0^1 girders were changed when the additional six collector lanes were constructed in 1965. These no longer have a welded cover plate detail and so were not considered in the measurement scheme.

Although it was believed that the welded cover plate details would be fatigue-sensitive, it was decided that a direct comparison of the stresses in another type of structure would be quite useful. The collector lanes are supported by continuous girders where the stress history in one span can be significantly influenced by a load in another. For this part of the investigation, the eight girders supporting the eastbound collector lanes on the bridge were designated A, B, . . . , and H from north to south. Figure 1 shows all girder designations and cross sections of the superstructure in the test site.

PILOT TESTS FOR SELECTING CRITICAL LOCATIONS

All of the core lane girders in spans 1 to 6 except 0 and 0^1 contained the welded cover plate detail. The cover plates were not welded continuously but in a series of intermittent welds as shown in Figure 2. Because a comprehensive method of analysis was lacking at the outset of the investigation, the static and dynamic live-load stresses were not known for the individual girders or along the length of each girder. Thus, the critical fatigue stress regions could not be determined a priori. To determine the most highly stressed locations, a two-phase preliminary deflection survey was initiated.

Phase 1

Phase 1 was carried out with the ministry's structural research test vehicle (Fig. 3) loaded to a gross weight of 112,000 lb (50 000 kg). During this pilot test, the core lanes were closed to normal traffic and the bridge was traversed by the test vehicle that traveled in different lanes at two different speeds.

The deflectometers used consist of a thin wire rope firmly attached to the girder at one end and to the measuring head at the other end (Fig. 4). The measuring head is a metal tripod that rests on the ground and is connected to the wire rope through a strain-gauged cantilever. Tension in the rope is maintained with a brass weight. The deflection of the structure is then proportional to the measured strain of the centilever and can be calibrated.

The eastbound approach to the bridge is downhill and is somewhat rougher than the westbound; thus, most of the deflectometers were distributed on the girders of the eastbound core lanes. For comparison, however, three were placed under the westbound lanes. The distribution of deflectometers is given in Table 2.

Maximum deflection at each station as read from the calibrated oscillogram for each run is given in Table 3, which reveals several important facts:

1. There is little effect on the structure of the eastbound lanes by westbound traffic and vice versa.
2. The eastbound lane structure tends to deflect more than the westbound lane under nominally similar dynamic conditions. This phenomenon is believed to be associated with the difference in surface roughness.

3. As expected, girder 1 in spans 5 and 6 deflected most when the test vehicle was in the most southerly lane (runs 4 and 7, stations 8, 9, 10, and 11) because this girder is located under the right edge of the driving lane. Girder 2 is between the two right-hand lanes and, therefore, experiences equal deflection (station 5, runs 4, 5, 7, and 8). Girder 3 is under the middle lane and experiences the greatest deflection for middle-lane traffic (runs 5 and 8, stations 4 and 6).

From these considerations it was concluded that girder 2 is likely to be the most frequently and highly stressed of all the girders because it is located beneath the two right-hand eastbound lanes, which usually carry 98 percent of the heavy vehicles.

Phase 2

The second phase consisted of a continuous 2-hour monitoring of girder deflections caused by normal traffic flow. For this survey, the deflectometers were moved to new locations to concentrate on those girders that were discovered to be most active in phase 1. Three deflectometers were placed on the collector lane structure toqualitatively assess the difference in behavior between the two types of construction. The distribution of deflectometers for phase 2 is given in Table 4.

Results from the continuous monitoring confirmed an earlier observation that girder 2 experiences the most severe stressing. Figure 5 shows typical time histories (histograms) of the deflections measured during heavy vehicle passage in (a) core lanes where the maximum deflection occurs at station 5 and is about 0.164 in. (4.17 mm) and deflection at station 2 is almost as great with 0.156 in. (3.96 mm) and (b) collector lanes, which are continuous girder structures (as opposed to simply supported girders). There is an obvious coupling across the supports shown by the out-of-phase displacements of spans 5 and 6. Table 5 gives the maximum normal road traffic displacement measured at each station.

Girder 2 was expected to experience the most severe stress history. An approximate calculation of stress from deflections indicated that span 6 was expected to result in values about as high as those for spans 1 and 2, and, therefore, it was decided to investigate and monitor the three spans by using strain gauges and a magnetic tape recorder.

Twenty locations in the core lane structure and four on the collector girders were instrumented (Fig. 1). Not all of these were needed for the stress measurements; however some duplication was necessary to cover for the eventuality of gauge failures and also to allow for the possible investigation of spatial anomalies that might arise during testing.

Each strain gauge station was identified by a three-character alpha-numeric code. The first is a number designating the span. The second designates the beam and can be a number (core lanes) or a letter (collector lanes). The third is the number 1, 2, or 3 and defines the location on the beam. Number 1 designates midspan or the point of highest bending moment. Number 2 designates a station on the cover plate a few inches from its end. Number 3 designates a position on the base material 4 in. (101.6 mm) from the end of the cover plate. Table 6 gives all strain gauge stations.

STRAIN GAUGE INSTRUMENTATION AND TECHNIQUES

Strain gauges used in the instrumentation were Micro-Measurement's EA-06-250-TG-350. The adhesive used was Micro-Measurement's AE-10, and the waterproofing compound was Automation Industries' GW-5.

The strain gauges were initially bonded with AE-10 to a 4-in.-wide (102 mm) strip of carrier material (Dupont Polymide Kapton 200H), which had been previously abraded. The gauges were wired in the full bridge configuration (Fig. 7) and waterproofed by a layer of GW-5 approximately $\frac{1}{8}$ in. (3.18 mm) thick. These patches were trimmed to 3 by 3 in. (76 by 76 mm) and installed at previously described locations on the steel girders with AE-10 adhesive, pressure pads, and heat lamps as shown in Figure 6.

A six-lead-wire system was used with two wires each for excitation, signal, and shunt calibration (Fig. 7).

Table 4. Placement of deflectometers (phase 2).

Station	Span	Beam	Position on Beam
1	1	2	Eastern end of cover plate
2	1	2	Midspan
3	1	2	Western end of cover plate
4	5	3	Midspan
5	5	2	Midspan
6	5	A	Midspan
7	—	—	—
8	5	D	Midspan
9	6	D	Midspan
10	5	2	Eastern end of cover plate
11	5	2	Western end cover plate

Table 5. Maximum deflections during 2-hour normal traffic period.

Station	Maximum Deflection (in.)	Station	Maximum Deflection (in.)
1	0.266	7	—
2	0.295	8	0.246
3	0.276	9	0.158
4	0.197	10	0.207
5	0.325	11	0.276
6	0		

Note: 1 in. = 25.4 mm.

Table 6. Strain gauge stations.

Span 1	Span 5	Span 6
121	511	611
122	521	621
123	522	622
131	523	623
	531	631
	532	632
	533	633
	541	641
	5E1	6E1
	5E3	6E3

Figure 5. Typical road traffic girder deflections.

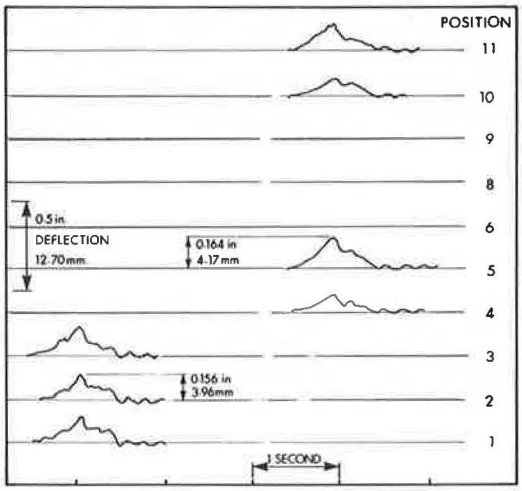

(a) HEAVY VEHICLE IN CORE LANES

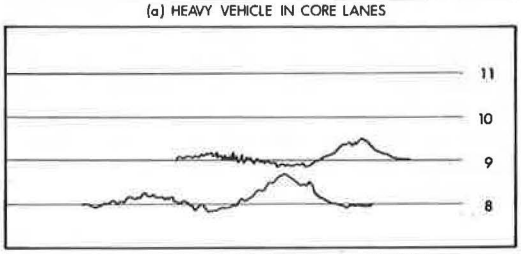

(b) HEAVY VEHICLE IN COLLECTOR LANES

Figure 6. Strain gauge application.

The excitation, signal conditioning, and amplification for the strain gauge bridges were supplied from an Endevco system, and the resulting signals were recorded on a seven-channel Philips Anal-Log 7 tape recorder. Calibration and zero balance adjustments were made every 12 hours during recording. The Endevco system has provision for inserting shunt calibration resistors. Suitable resistors were inserted to give calibrations of 200, 100, and 50 μin./in. (41.37, 20.68, and 10.34 MPa).

The required values of calibration resistor are calculated from the formula

$$\text{Calibration resistance} = (\text{gauge resistance}) \times \left[\frac{10^6}{\text{gauge factor} \times \text{microstrain} \times A}\right]^{-1.0}$$

where A is a bridge gain of 2.6 for the full bridge configuration used.

The resistors used were Welwyn type M22D (temperature coefficient of 100 parts per million) and had values of 316,634 and 1270 kΩ to give the required calibrations of 200, 100, and 50 ± 1 percent in all cases.

SYSTEM TEST

Before magnetic tape recordings were begun, the strain gauge bridges were tested again with the oscillograph. A continuous recording for 1 hour was taken for each of the 24 strain gauge stations. It was found that all 24 installations were functioning satisfactorily and that each channel yielded an electronically clean and useful signal. It was decided from the preliminary deflection tests that a 200-μin./in. strain or 6,000 psi (41.37 MPa) was the maximum to be expected and that this should be used as both a maximum calibration value and a full scale for the recordings. The system test confirmed this assumption.

STRAINS FROM PASSAGE OF A VEHICLE OF KNOWN WEIGHT

The test vehicle with a gross weight of approximately 84,000 lb (38.8 tons) was driven in normal traffic. (No attempt was made to identify the nature and distribution of commercial traffic; for obvious reasons the Toronto Bypass does not readily lend itself to such an enterprise.) The vehicle's passing time was synchronized with the tape recorder by means of a three-way radio communication. Use of the tape recorder enabled the data to be analyzed later. A total of 18 vehicle passes or runs were made.

Table 7 gives the maximum strains experienced by the bridge structure during the vehicle passage for the core lanes, and Table 8 gives those for the collector lanes.

The tabulated strains are estimated to be accurate to within approximately ±5 μin./in. or 150 psi (1.03 MPa), which allows for equipment error and manual trace interpretation. In all cases, a positive strain is tensile and a negative one compressive. The values given in Tables 9 and 10 are strictly maxima and do not give any indication of variation with time.

Figure 8 shows the core lane strain histories of stations 123 and 623 for run 8. These traces are typical of the core lane strains recorded during normal traffic flow. In some cases a slight vibratory motion was apparently induced. The preliminary study had indicated that the high-speed passes tended to yield higher deflections than the pseudostatic passes. This trend was much reduced in the strain measurements. There appeared to be little forced vibration except for the thump effect caused by the rough approach. This effect did not vary appreciably within the speed range observed.

Figure 9 shows typical strain histories for the collector lane structure. The strain gauges located on the thinned-down portion of the flange show tensile and compressive peaks in sequence. This reflects the interspan influence made possible by the continuous nature of the girders over the supports.

As in the core structure, the effect of vehicle velocity on vibration was minimal, which indicates the absence of significant forced responses. Nevertheless, the continuous structure seemed to indicate higher dynamic responses than the comparable simply supported ones that carried the core lanes.

Figure 7. Strain gauge wiring.

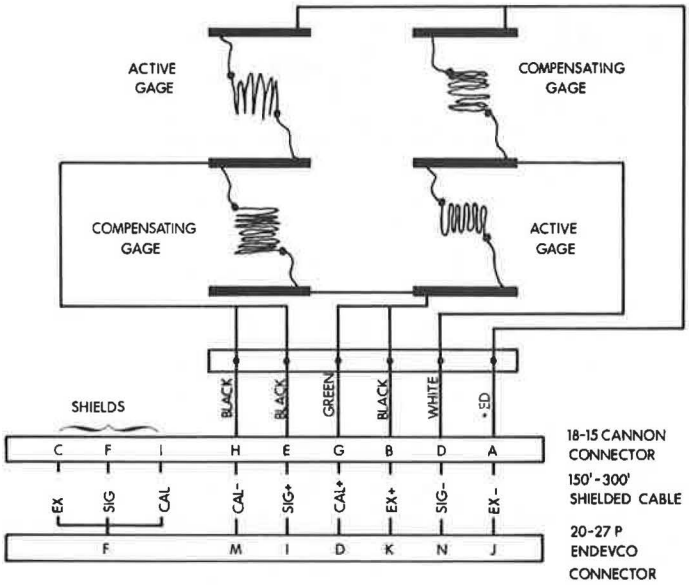

Table 7. Peak strains during passage of test vehicle (core lanes).

Run Number	Measured Strain (μin./in.) for Station						
	123	121	523	521	531	623	621
2	85	69	55	57	33	59	54
4	76	58	58	54	54	54	53
6	21	21	20	20	35	21	18
8	85	82	48	67	37	45	60
10	72	57	50	54	60	84	68
12	30	30	31	32	53	28	22

Note: 1 μin/in. = 0.2068 MPa.

Table 8. Peak strains during passage of test vehicle (collector lanes).

Run Number	Measured Strain (μin./in.) for Station			
	5E3	5E1	6E1	6E3
13	15	-19	-18	-19
	-12			21
14	67	-64	-81	-77
	-49			100
15	40	-39	-49	-51
	-30			55
16	15	-22	-28	-32
	-15			29
17	69	-78	-87	-85
	-64			117
18	38	-41	-50	-59
	-29			53

Figure 8. Test vehicle induced strains at two core lane structures (run 8, Table 8).

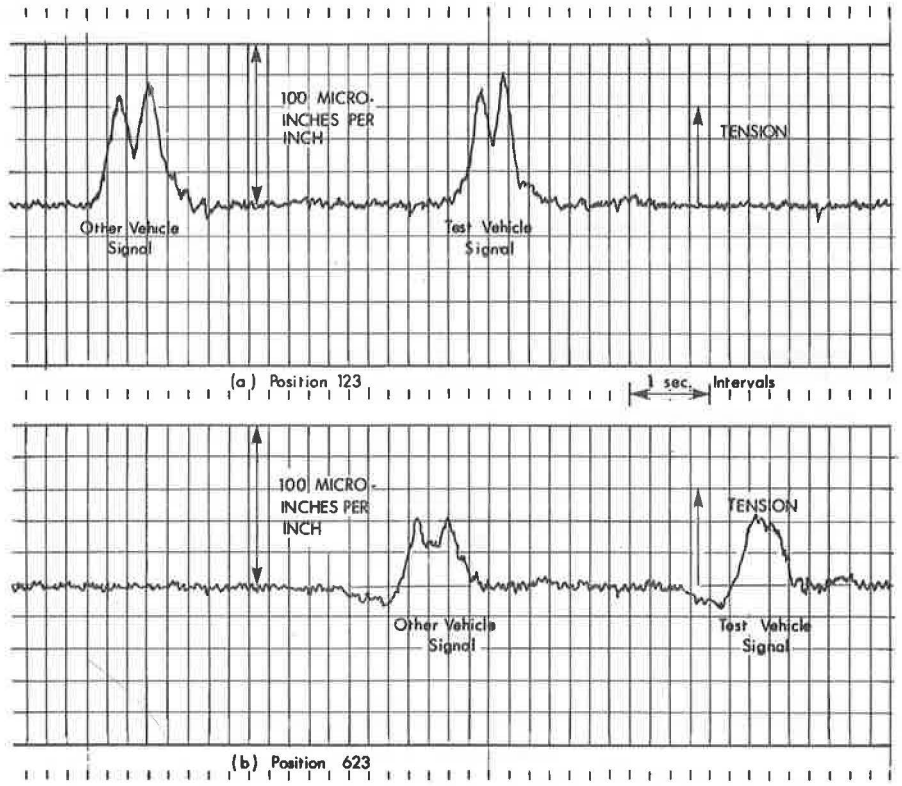

Figure 9. Test vehicle induced strains at two collector lane structures (run 17, Table 8).

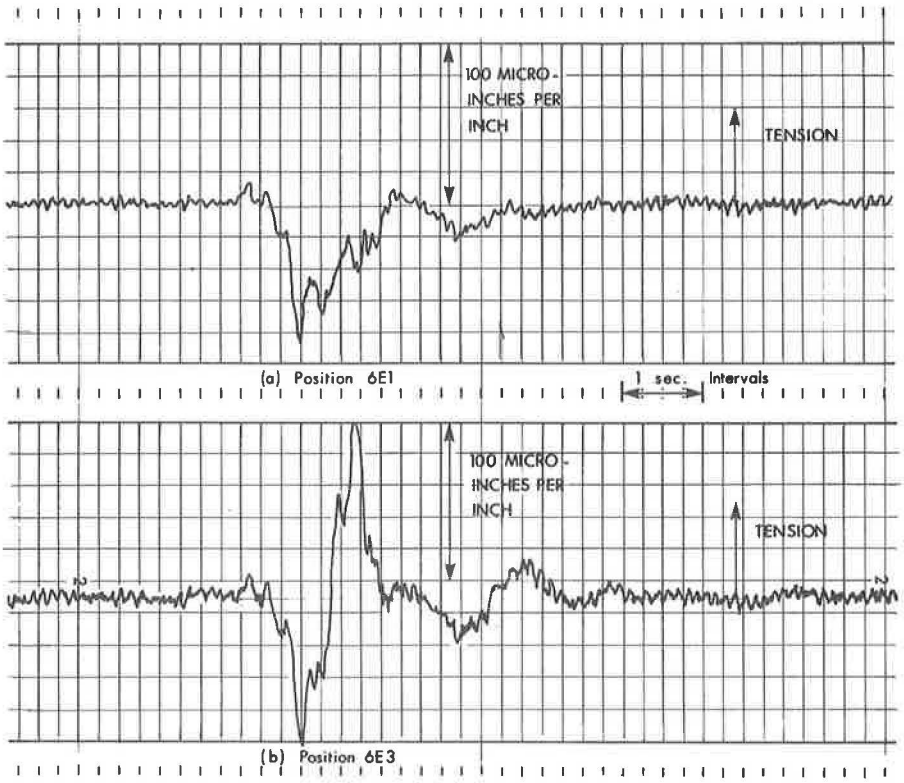

CONTINUOUS STRAIN RECORDINGS

The continuous recording of strain began at the end of February 1972. Seven channels were recorded simultaneously. A calibration signal was recorded on each channel at the beginning of each tape for about 1 min. This was repeated at the end of the tape. All recording was carried out at the minimum recorder speed of $^{15}/_{16}$ ips (23.8 mm/s), and this resulted in a 12-hour recording for each reel of tape. The highest frequency expected in the signal was less than 5 Hz (Figs. 8 and 9), and the frequency response of the tape recorder was quite adequate at that low speed. All recordings were made in the FM mode because of the predominant low frequency of the signal.

For most of the recording session, the seven stations monitored had been found to be most severely stressed in the preliminary and system test programs. Some recordings, however, were made with signals from other stations, which were combined into groups 1 and 2.

It was decided to attempt to analyze data soon after recording and to reuse the tapes so that the required inventory of magnetic tapes could be kept to a reasonable minimum and recording continuity could be maintained. A comparison of data blocks showed that the daily traffic patterns of the Toronto Bypass are homogeneous enough to consider all data as coming from a single sample.

DATA ANALYSIS

From the preliminary tests and the playback of the continuous records, it became apparent that the strain history was nonstationary. This precludes the more conventional means of measurement and dictates a statistical analysis.

Several parameters, such as fluctuating and mean stresses, fabrication techniques, and material, influence the fatigue life of structures. There is some indication that mean stress plays a minor role in typical materials used for built-up bridge structures that are loaded to fairly high stress levels (2). This may not be true with lower stress levels and a large number of applications. The effect of alternating stress is quite well understood for constant strain or stress fluctuations that are sinusoidal in waveform. If the time history is random in nature, stationary, and narrow banded, then the fatigue characteristics are more complex. The primary parameter, however, is the stress root-mean-squares (e.g., 3). As the bandwidth increases there is some indication that the statistical properties of the rises and falls (i.e., the magnitude of the difference between a maximum and the previous or succeeding minimum) govern fatigue characteristics (4).

Because the girder strain histories were neither sinusoidal nor stationary, a simple frequency-amplitude relationship could not be found. Therefore, calculation of the statistics of the amplitude, the maxima (peaks and troughs), and the excursion (rises and falls) would be necessary for a fatigue life assessment.

The University of Toronto computer research facility contains an eight-channel A-D interface to its IBM 360/44 digital computer. The digitizing rate is at an adequate level of 20,000 per second total for all channels. The rate chosen for the analysis was 1,250 per second per channel. Figure 10 shows an oscillograph trace at low and high paper speeds of a typical vehicle passage. A sample rate of 1,250 per second on data analysis is equal to approximately 40 per second in real time. In the lower part of Figure 10, this rate corresponds to one sample per division on the time scale, and this can be seen to give excellent resolutions or signal reproduction.

When each reel of analog tape had been digitized, it was analyzed with the IBM 360/44. The analysis consisted of several steps, which are shown in Figure 11. The data, as read by the computer, were not normalized. The calibration level and signal zero for each channel at the beginning of each tape were evaluated manually with a digital voltmeter, and these were used as input in the analysis program as initial normalizing values.

The calibration signal was rechecked at the end of each reel. In all cases it was unchanged. The signal zero, however, did change at times, which was felt to be due to (a) electronic drift, (b) temperature effects in the bridge, and (c) static load change caused, for example, by an accumulation of snow and debris on the deck during the winter.

Figure 10. Typical vehicle strain history at low and high paper speeds for sample rate determination.

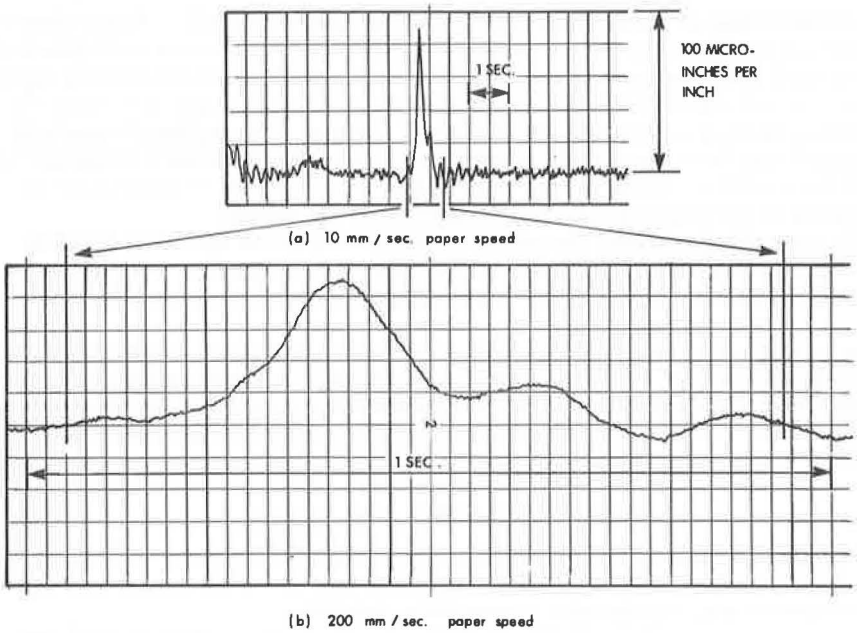

Figure 11. Flow chart for computer analysis of digitized data.

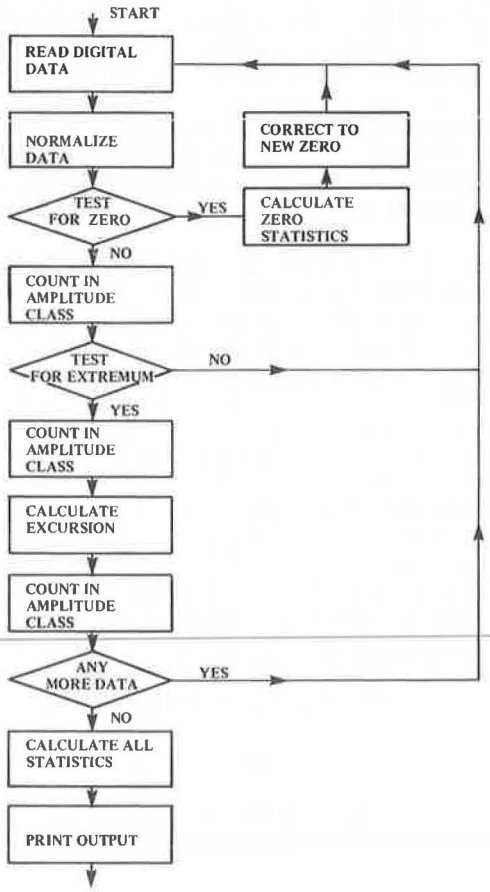

The signal zero used to compensate for these effects in normalizing was continuously updated by using the average of near zero samples. A sample was arbitrarily eliminated from the main statistical analysis if it fell between -5 and +5 μin./in (1.03 MPa) when normalized by the current factors. The mean and standard deviation of these samples were calculated as a safeguard against malfunction.

All nonzero samples, peaks, troughs, rises, and falls were tabulated by class in 5-μin./in. (1.03 MPa) increments. The mean and standard deviations for each quantity were also calculated.

The computer output on analysis consisted of one table for each channel that gave a class by class breakdown of the various statistics and a summary page listing the total counts and calculated statistics. Figure 12 shows the definition of various terms of reference used in the statistical analysis.

EXPERIMENTAL RESULTS AND DISCUSSION

The first 24 hours of recording were of group 1 stations 121, 123, 521, 523, 531, 621, and 623. All seven channels were analyzed for a direct comparison between stations. The next 24 hours of recording were of group 2 locations, and again all seven were analyzed.

Figure 13 is a typical amplitude plot for group 1 stations during one 12-hour period. A comparison between stations revealed that station 123 was highest; 121 was next. Stations 521 and 621 were almost identical and were lower than 121.

A comparison between group 2 stations revealed that 511 was almost equal to 121 and that all the others were considerably lower. On the basis of these comparisons, it was decided for the remainder of the analysis to concentrate on 123, 521, and 621 as being representative of the most highly stressed locations.

Design stress values were calculated for station 123. Note that the core structure was designed as noncomposite; however, the channel type of shear connectors were provided, and the structure is believed to behave as at least partially composite for live loads. Bottom fiber stresses determined by using AASHTO specifications are (a) dead load—7.67 ksi or 256 μin./in. (53.9 MPa), (b) live load (noncomposite)—10.67 ksi or 356 μin./in. (73.5 MPa), and (c) live load (composite)—8.24 ksi or 275 μin./in. (56.9 MPa).

One can observe later that, assuming composite action, the maximum observed stress does not exceed 50 percent design live-load stress. This situation is believed to be common in all girder types of bridges designed in accordance with the AASHTO specifications and not particular to this structure.

The overall average number of samples in each 5-μin./in. (1.03 MPa) amplitude range per hour for stations 123 and 621 are shown in Figures 14 and 15. These are based on 133.63 hours of data, which is less than the total recorded.

The data (Figs. 14 and 15) are not true probability values because they have not been normalized. To find probability, one must divide by the total number of samples per hour (e.g., 1,250 × 3,600/32). This, however, results in extremely low probabilities in all regions except amplitudes near zero and is a valid situation because most of the time the strain values are near zero. For more meaning, the probability should be expressed in terms of a sample falling in a given range during the passage of a heavy vehicle. This is a complex joint probability because it involves the distribution of vehicles with time, the weight distribution with vehicles, and random lateral positioning of the vehicles.

A simpler, more intuitive approach can be used if it is assumed that the amplitude distribution is made up of samples from two populations (Fig. 16). One set of values is very narrow in the amplitude direction but contains a great many samples. This implicitly takes account of electronic noise plus the passage of passenger cars and light commercial vehicles. The other population is interesting for fatigue life assessment because it gives the probability of having a given strain amplitude during the passage of a heavy vehicle.

An approximation to this ideal approach implied the arbitrary rejection of data in the -5 to +5 amplitude range. The normalizing factor is then the total number of samples considered, and this results in a probability density curve that is displaced vertically but that is otherwise identical in shape to the amplitude distribution curve (Fig. 13).

Figure 12. Data analysis terminology.

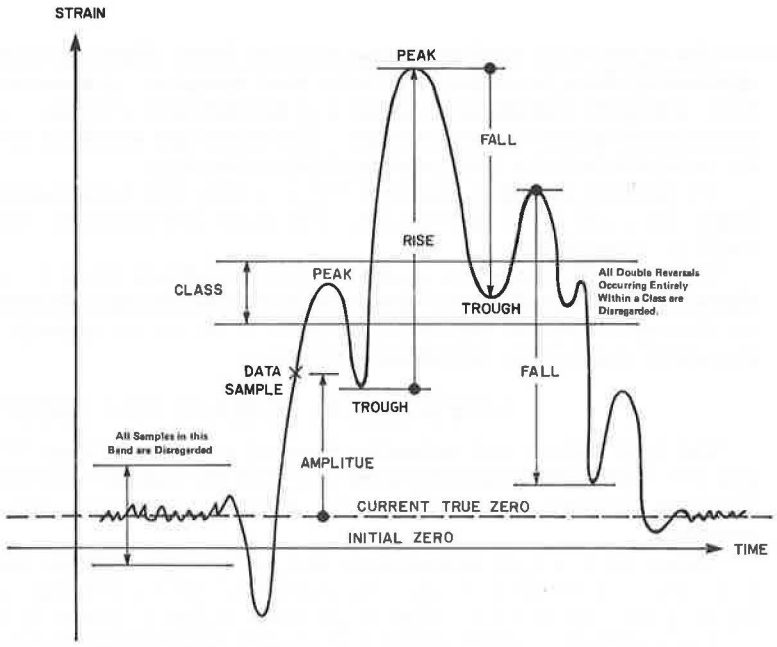

Amplitude: the instantaneous value of a variable or quantity.

Peak (Trough): a local maximum (minimum).

Rise (Fall): the difference in amplitude between a peak and the preceding (succeeding) trough.

Class: a band of arbitrary width within which all data points are considered to have equal amplitude.

Figure 13. Strain amplitude distribution for station 621 for 11.5 hours.

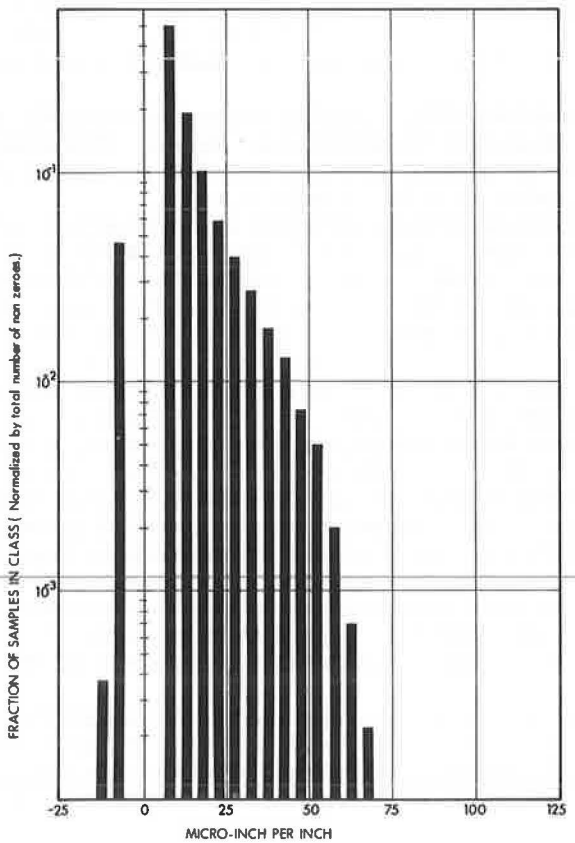

Figure 14. Strain amplitude distribution of average number of samples per hour at station 123.

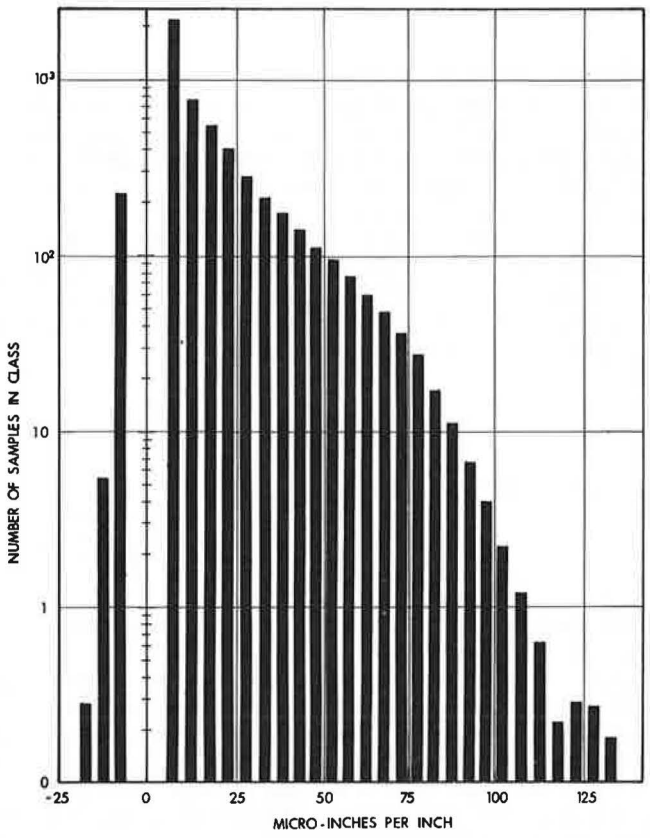

Figure 15. Strain amplitude distribution of average number of samples per hour at station 621.

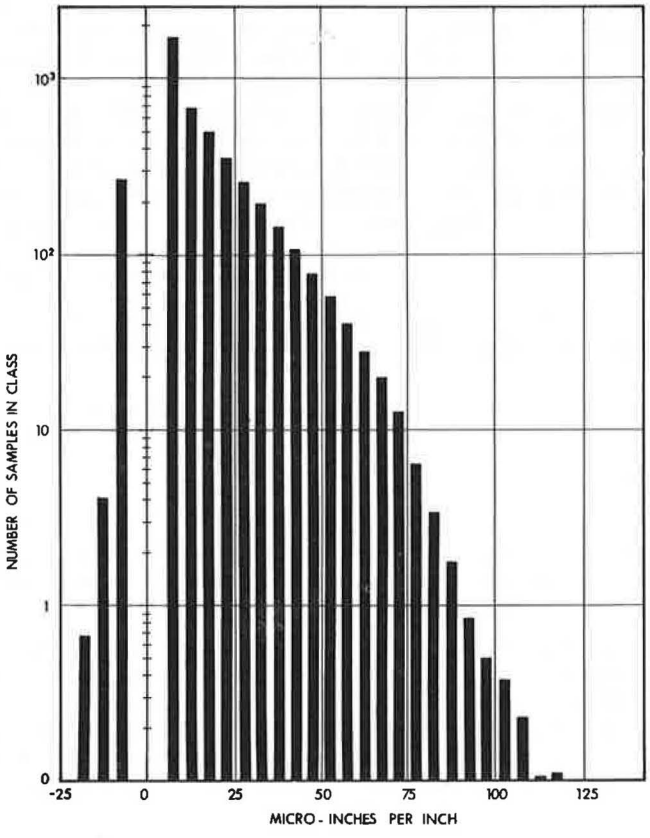

The distributions of maxima (peaks) and minima (troughs) per hour for station 123 are shown in Figures 17 and 18. As in the case of the amplitude distributions, these are not probability curves and the same considerations apply.

The distributions of excursions with amplitude are shown in Figures 19 and 20. The average hourly number of rises and falls of a given amplitude are shown, and these are almost identical to the individual quantities.

In addition to the distributions of amplitudes, extrema, and excursions, the mean and root-mean-square values are necessary for an assessment of the fatigue life. These quantities can be calculated from the distribution in the following manner: Let a_i be the amplitude of the ith sample of the variable being considered and N be the total number of samples. Then the mean value is

$$\frac{\sum a_i}{N} = a$$

and the root-mean-square is

$$\sqrt{\frac{\sum (a_i - a)^2}{N}}$$

These quantities are given in Table 9 for the strain amplitude and excursions for the three critical locations.

The stress levels for the fatigue tests in Fisher et al. (2) for partial length cover plates were those on the bottom of the tension flange on the base metal at the end of the cover plate. This is exactly the configuration for station 123 in the present investigation, and, therefore, a direct comparison should be possible. However, the minimum stress range used in testing (2) was 6,000 psi (41.37 MPa), and this resulted in a life of some 7×10^6 cycles. Figure 17 shows that a stress peak of 125 μin./in. or 3,750 psi (25.85 MPa) can be expected at station 123 about once every 10 hours. A pair of excursions of that amplitude is expected about once every 24 hours (Fig. 19).

With the length of sample taken for this investigation, it is felt that the statistics are reliable to levels of extrema and excursions occurring once in 10 hours with reasonable extrapolation to once in 100 hours. As indicated above, however, even at these low levels of expectation, the measured stresses are lower than the minimum values used in other tests (2). Because of this large difference in level and of the additional major dissimilarity in waveform between the measured stresses of the Leslie Street overpass and the reported fatigue tests, a reliable quantitative prediction of fatigue life cannot be obtained. Nevertheless an attempt was made to estimate the expected fatigue life of the core lane structure by using Miner's hypothesis.

APPLICATION OF MINER'S HYPOTHESIS

Miner's hypothesis was used to evaluate the effect of cyclic stressing of a random nature on metals. It is postulated by the following equation:

$$\sum_i \frac{n_i}{N_i} \leq 1.0$$

where

- i = index for stress range,
- n_i = number of expected cycles of stress range S_i, and
- N_i = number of cycles of stress range S_i so as to cause fatigue failure as established by laboratory testing.

As a part of this investigation, the intermittent welds were exposed by sandblasting and later were inspected at many locations selected at random. No signs of fatigue cracks were found at any of these locations. This, in addition to the generally low stress levels observed, seems to indicate that the Leslie Street bridge is by no means a critical case and no great harm can be done by applying the hypothesis to the available data.

Figure 16. Schematic example of addition of overlapping distribution.

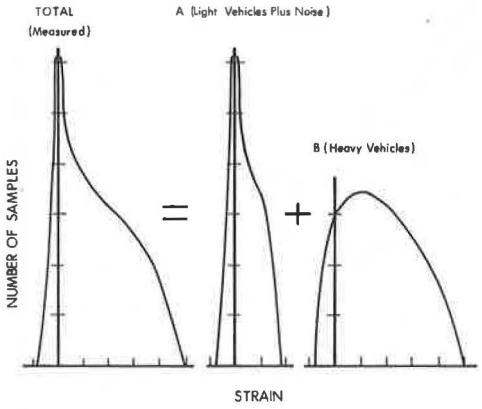

Figure 17. Distribution of average number of maxima per hour at station 123.

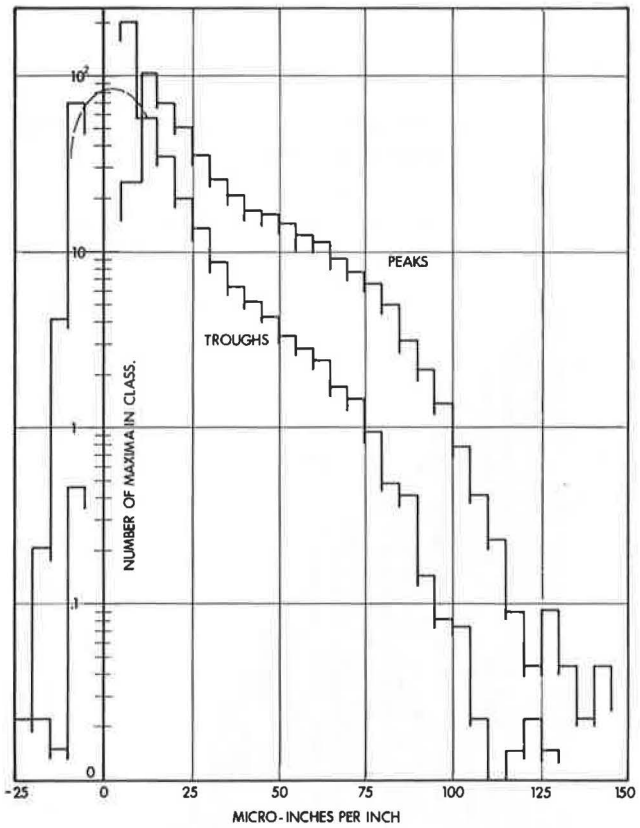

Figure 18. Distribution of average number of maxima per hour at station 521.

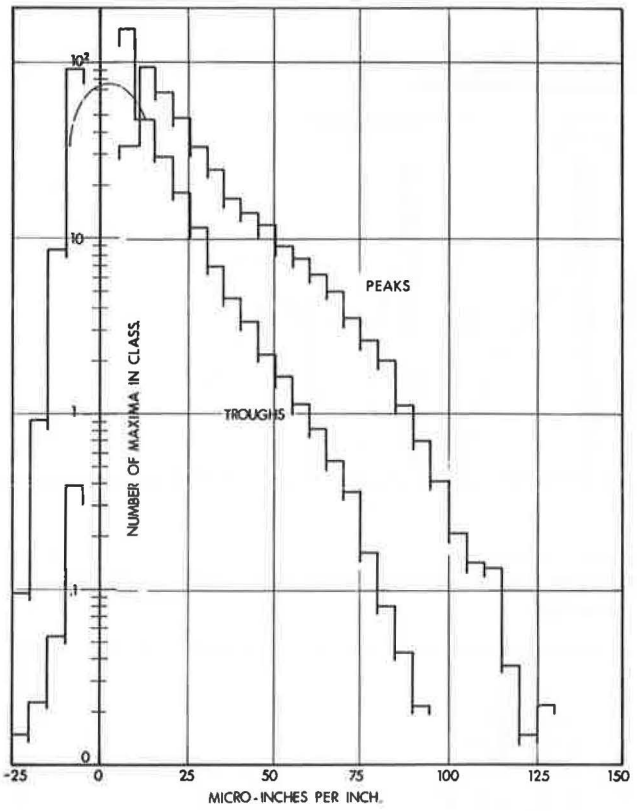

Figure 19. Distribution of average number of rises and falls per hour at station 123.

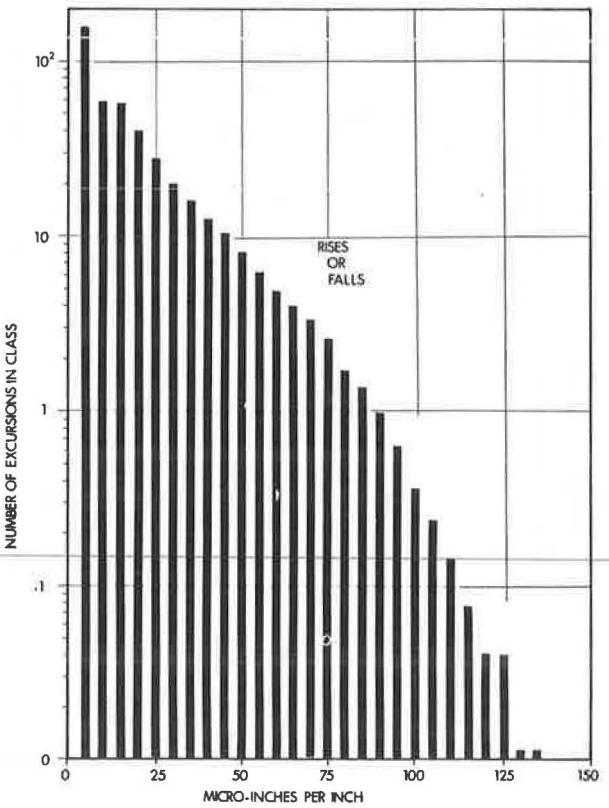

Figure 20. Distribution of average number of rises and falls per hour at station 521.

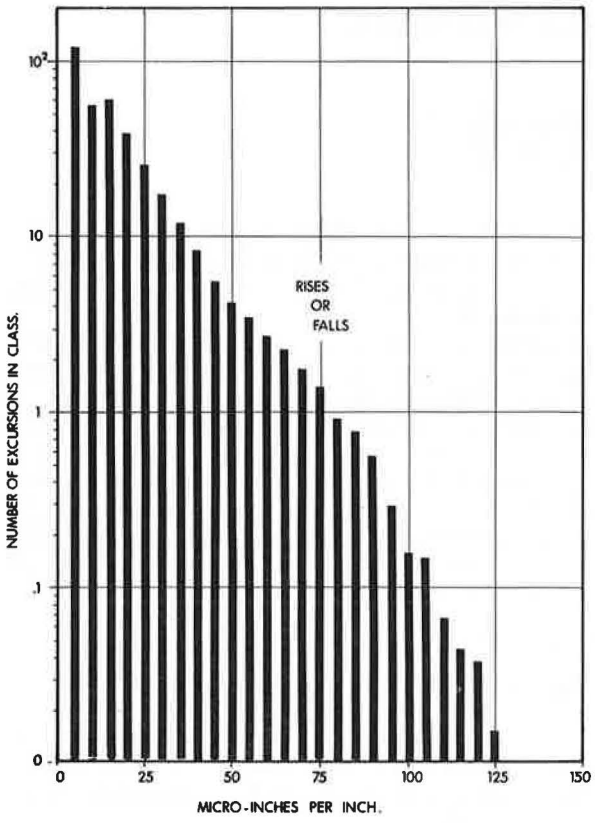

Table 9. Calculated mean and rms strains.

	Strain Amplitude (μin./in.)		Excursions (μin./in.)	
Position	Mean	RMS	Mean	RMS
123	18.6	17.4	18.5	17.5
521	16.4	14.9	17.0	15.1
621	16.4	14.0	18.1	16.2

Figure 21. Mean fatigue strength and 95 percent confidence limits for rolled, welded, and cover-plated beams.

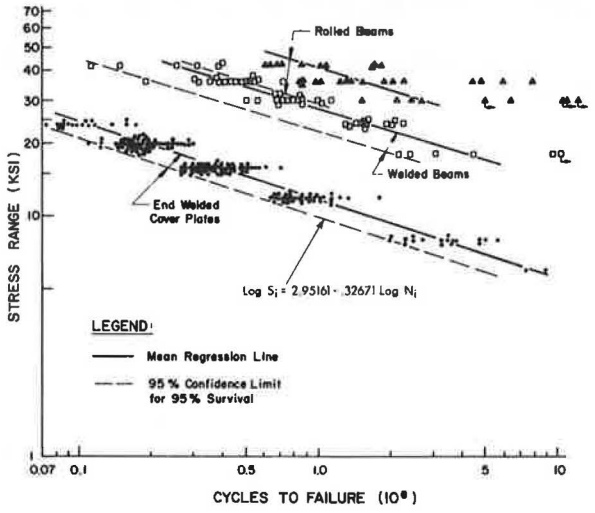

Table 10. Evaluation of data.

Location	Expected Life (years)
123	302
521	492
621	557

For this application the representative lower bound S_i - N_i curve (95 percent confidence limit for 95 percent survivals, 2) was used (Fig. 21). The equation is

$$\log S_i = 2.95161 - 0.32671 \log N_i$$

or

$$N_i = \left(\frac{894.56}{S_i}\right)^{3.06082}$$

where S_i is given in ksi.

All data for this relationship were obtained for stress levels higher than 6,000 psi (41.37 MPa) and had to be extrapolated for the 0 to 4,000 psi (0 to 27.57 MPa). The validity of this extrapolation is questionable. Table 10 gives a summary of the evaluation based on 6-day weeks on a year-round basis.

If one accepts these figures for the expected life only as indicative, the margin of safety against fatigue failure still appears to be excessive. The discrepancy originates from the fact that the fatigue consideration is applied to the design live-load stress (AASHTO specifications). When one reviews the available stress history data gathered by various agencies during the past few years, it becomes evident that in reality either design stress does not occur at all or it occurs with such a low frequency that the development of any fatigue situation is precluded. The phenomenon is associated with the low probability of the simultaneous, multiple presence of vehicles on a structure. Because the problem is statistical in nature, its recognition appears to be in conflict with the prevailing concept used in fatigue consideration of highway bridges.

REFERENCES

1. Cudney, G. R. Stress Histories of Highway Bridges. Jour. Structural Division, Proc. ASCE, Dec. 1968.
2. Fisher, J. W., Frank, K. H., Hirt, M. A., and McNamee, B. M. Effect of Weldments on the Fatigue Strength of Steel Beams. NCHRP Rept. 102, 1970.
3. Swanson, S. R. Random Load Fatigue Testing: A State of the Art. Materials Research and Standards, Vol. 8, No. 4, April 1968.
4. Rice, J. R., Paris, P. C., and Beer, F. P. On the Prediction of Some Random Loading Characteristics Relevant to Fatigue. In Acoustical Fatigue in Aerospace Structures, Syracuse Univ. Press, 1965.
5. Bendat, J. S., and Piersol, A. G. The Measurement and Analysis of Random Data. John Wiley, 1966.
6. Fatigue Strength of Welded Steel Beams. NCHRP Research Results Digest 44, March 1973.
7. Bowers, D. G. Loading History, Span No. 10 Yellow Mill Pond Bridge, I-95, Bridgeport, Connecticut. Connecticut Dept. of Transportation, Jan. 1973.

BRIDGE FATIGUE DUE TO DAILY TRAFFIC

Conrad P. Heins, Jr., Department of Civil Engineering, University of Maryland; and C. F. Galambos, Federal Highway Administration

This paper presents a summary of loading history studies that have been conducted on girder-slab bridge structures. Characteristics of the bridges, bridge locations, and loadings are examined to present uniform code criteria. A technique that considers random load application is presented for possible design consideration. The method incorporates distribution of truck type, location of road, simple and continuous spans, and probable induced field stresses.

•DURING the past 5 years, various universities and state and federal highway agencies (1, 2, 3, 4, 5, 6, 7, 8, 9, 10) have conducted cooperative field studies to determine the loading history of bridge structures. These tests have provided information on the magnitude of induced bridge girder stresses and the vehicles that induce these stresses.

A thorough study of these data shows that the induced live-load stress ranges are low (1.0 to 3.0 ksi) in comparison with the design live-load stresses. This then suggests that the present fatigue design criteria may be too restrictive and some revision might be in order. The design guides also should account for the characteristics of the actual vehicles that traverse the bridges, as well as the random nature of the loads.

Therefore, it is the intention of this paper to present one possible method of fatigue design that does consider random load characteristics and actual induced stresses.

VEHICLE CHARACTERISTICS

During the various load history tests, classification counts were made of truck types crossing a bridge structure. If the structure was near a weighing or loadometer station, the gross weight, weight distribution, and axle spacings of the vehicles were also obtained. Data collected during the bridge tests in Alabama (1), Connecticut (2), Minnesota (3), Maryland (4, 5, 6, 7, 8), Michigan (9), and Virginia (10) are given in Tables 1 through 5. During many of these tests only classification counts were made.

The percentage of distribution of trucks for the various bridge tests is given in Table 1. The classifications are based on five truck types (Fig. 1). Although some reports list other truck types, most can be categorized under these five classes. Table 1 also gives the type of road system associated with each test. These data suggest that road systems can be divided into three classifications: metropolitan, urban, and rural. An average of the data for these classifications is given in Table 2. This distribution would then be used, instead of more reliable data, for fatigue analysis.

Table 3 gives the mean gross weights for five truck types and bridge tests. The ranges in gross weights are used to tabulate induced girder moments for each truck type.

Table 4 gives the percentage of the total load distributed to each axle for the various truck types. Only the tests conducted in Maryland and Connecticut provided such information. The average of these values will be used for describing typical vehicles.

Table 5 gives the average spacing between axles for the various truck types. Data were obtained from tests conducted in Virginia, Maryland, and Connecticut.

By using the resulting data from Tables 4 and 5, one can develop typical trucks

Publication of this paper sponsored by Committee on Dynamics and Field Testing of Bridges.

Table 1. Percentage of distribution of trucks by test site.

Test Site	Truck Type 2D	3	2S-1	2S-2	3S-2	Total Trucks per 24 Hours	Classification[a]
Ala. 1	26.3	14.3	4.4	21.2	32.8	570	Rural, S
Ala. 2	23.2	5.3	3.3	15.4	52.8	1,090	Rural, I
Conn.	20.4	3.4	3.95	30.9	41.7	5,416	Urban, I
Minn.	31.0	27.1	2.5	5.8	33.6	2,551	Metropolitan, I
Md. 1	17.2	1.3	7.9	29.0	44.6	782	Rural, I
Md. 2	15.3	1.5	7.2	30.0	46.0	940	Rural, I
Md. 3	38.1	19.6	8.9	15.6	17.8	1,528	Metropolitan, I
Md. 4	19.8	5.9	6.7	21.3	46.3	1,468	Rural, S
Md. 5	26.8	6.2	5.6	20.8	40.6	542	Rural, S
Md. 6	27	11	5	18	39	925	Rural, S
Mich. 1	15	2.1	16.8	43.6	22.5	600	Rural, S
Mich. 5	11.9	2.2	17.5	34.6	33.8	690	Urban, S
Mich. 7	12.9	7.5	17.1	30.7	31.8	972	Urban, S
Va. 1	9.3	1.4	7.4	29.7	52.2	1,430	Urban, I
Va. 2	10.9	1.0	5.6	18.9	63.7	870	Urban, I

[a]S = state route, and I = Interstate.

Table 2. Percentage of distribution of trucks by road type.

Truck Type	Road Type Metropolitan	Urban	Rural
2D	35.0	13.0	21.0
3	23.0	3.0	6.0
2S-1	6.0	10.0	7.0
2S-2	11.0	30.0	25.0
3S-2	25.0	44.0	41.0

Figure 1. Truck types.

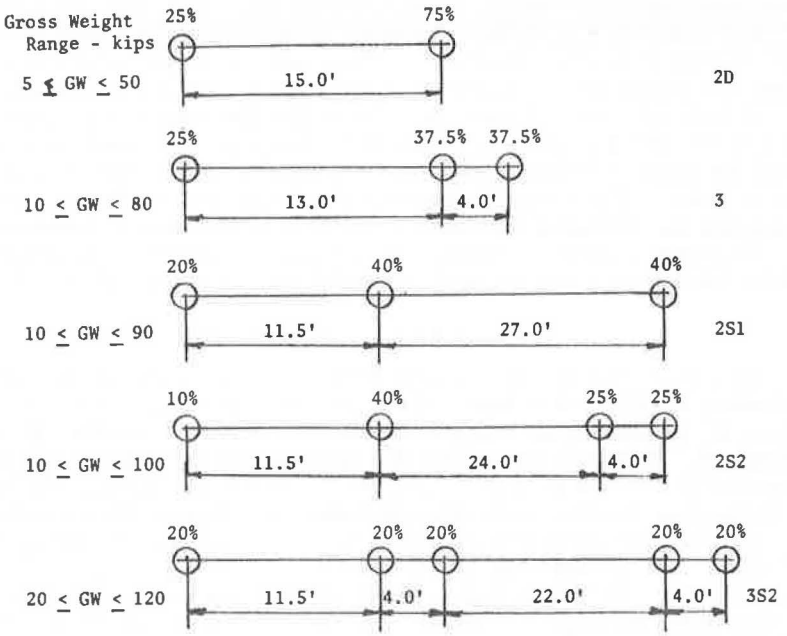

Table 3. Vehicle gross weight and standard deviation.

Item	Truck Type 2D	3	2S-1	2S-2	3S-2
Test site					
Va.					
Mean G	13.1	22.4	29.7	38.5	54.9
S	5.51	9.91	15.93	9.86	13.96
Mich.					
Mean G	15.0	—	36.6	37.0	48.7
S	5.0	—	9.7	13.0	13.7
Md. 1					
Mean G	14.7	32.4	31.4	43.2	56.6
S	6.32	12.89	9.67	15.19	19.79
Md. 2					
Mean G	13.0	48.0	29.8	38.0	53.0
S	—	—	—	—	—
Conn.					
Mean G	15.7	38.4	54.7	45.8	48.2
S	—	—	—	—	—
Average					
Mean G	14.3	35.3	36.1	40.5	52.3
S	5.6	11.4	11.8	12.7	15.8
Range	3 ≤ G ≤ 25.5	12 ≤ G ≤ 58.1	12 ≤ G ≤ 59.7	15 ≤ G ≤ 65.9	21 ≤ G ≤ 83.9

Note: G = gross weight, kips; and S = standard deviation.

(Fig. 1). This is necessary to determine probable induced girder moments caused by the five truck types.

SIMPLE SPAN STUDY

Relation of Induced to Design Maximum Moments

To relate the probable induced stresses from various truck types to the design stresses, relationships between induced maximum moments (M) and AASHTO live-load design maximum moments (M_A) have been calculated and tabulated. These values are given in Table 6 as a ratio of M/M_A for various truck types and the corresponding range in gross weights for the typical truck types. The length of spans ranges from 40.0 to 140.0 ft.

Reduction Factor

As noted previously, the observed stresses during the field tests were less than the design live-load stress. This is partly because of the truck types that induce these stresses as opposed to the standard AASHTO HS-20-44 truck and partly because of differences in load distribution, material properties, and the unaccounted-for contributions of automobiles and parapets. With this observation in mind, a study was conducted (11) to relate vehicle characteristics to corresponding induced stresses and bridge stiffness. The results of this study provided the following general equation:

$$(f_r)_{test} = \frac{A + B(G)}{S/12L} \tag{1}$$

where

$(f_r)_{test}$ = observed induced stress range at (a) centerline of the girder and (b) off the end of the cover plate,
G = vehicle gross weight,
S = girder section modulus,
L = span length in feet, and
A, B = constants obtained from linear regression analysis.

Centerline of Girder—A relationship between the induced stresses and design stresses for the centerline of the girder can be given by the following equation:

$$\frac{f_{test}}{f_{design}} = \frac{A + B(G)}{S/12L} \times \frac{S}{M\left(\frac{\bar{S}}{5.5}\right)(1 + I)} \tag{2}$$

where

M = calculated absolute maximum moment caused by a set of wheel loads of an AASHTO truck,
$\bar{S}/5.5$ = distribution factor,
$\bar{S}$ = girder spacing, and
$I = \text{impact factor} = \left(\frac{50}{L + 125}\right)$.

The AASHTO moment can be computed by M = (108L - 1,680) kip-in., where L = feet. Defining $\frac{f_{test}}{f_{design}} = F$ and substituting in the M equation gives

$$F = \frac{[A + B(G)]\,12L}{(108L - 1{,}680)\left(\frac{\bar{S}}{5.5}\right)(1 + I)} \tag{3}$$

Assuming that several trucks can occur on the bridge at the same time during the field

Table 4. Percentage of weight distribution by axle.

Truck Type	Axle A		B		C		Average A	Average B	Average C
	Md.	Conn.	Md.	Conn.	Md.	Conn.			
2D	25	41	75	59	—	—	33	67	—
3	25	33	75	67	—	—	29	71	—
2S-1	20	27	40	40	40	33	24	40	36
2S-2	10	19	40	36	50	45	14	38	48
3S-2	20	18	40	42	40	40	19	41	40

Table 5. Vehicle axle spacing.

Truck Type	Span A to B			B to C			Average A to B	Average B to C
	Va.	Md.	Conn.	Va.	Md.	Conn.		
2D	14	16	15.7	—	—	—	15.2	—
3	14	18	19.1	—	—	—	(13 + 4) or 17.0	—
2S-1	11.0	12	11.8	29.0	28.0	23.9	11.6	27
2S-2	11.0	12	12.1	27.0	28.0	28.7	11.7	(24 + 3.9) or 27.9
3S-2	12.0	12	11.1	30.0	30.0	33.3	11.7	(4.1 + 22 + 4) or 30.1

Table 6. M/M_A for a simple span bridge.

Truck Type	Gross Weight (kips)	Length (ft) 40	60	80	100	120	140
2D	20	0.365	0.327	0.312	0.304	0.299	0.296
	40	0.730	0.654	0.624	0.608	0.598	0.591
	60	1.096	0.981	0.936	0.912	0.897	0.887
	80	1.461	1.308	1.248	1.216	1.196	1.183
3	20	0.340	0.313	0.303	0.297	0.293	0.291
	40	0.680	0.627	0.606	0.594	0.587	0.582
	60	1.020	0.940	0.908	0.891	0.880	0.873
	80	1.360	1.254	1.211	1.188	1.174	1.164
2S-1	15	0.164	0.163	0.176	0.183	0.188	0.191
	30	0.327	0.326	0.352	0.367	0.376	0.382
	45	0.491	0.488	0.528	0.550	0.564	0.573
	60	0.654	0.651	0.704	0.734	0.752	0.765
	75	0.818	0.814	0.881	0.917	0.940	0.956
	90	0.982	0.977	1.057	1.100	1.128	1.147
2S-2	20	0.201	0.212	0.230	0.240	0.247	0.251
	40	0.401	0.424	0.460	0.480	0.493	0.503
	60	0.602	0.636	0.690	0.720	0.740	0.754
	80	0.803	0.847	0.919	0.960	0.987	1.006
	100	1.003	1.059	1.149	1.200	1.234	1.257
3S-2	20	0.199	0.208	0.229	0.241	0.248	0.252
	40	0.398	0.416	0.459	0.481	0.495	0.505
	60	0.597	0.624	0.688	0.722	0.743	0.757
	80	0.796	0.831	0.917	0.962	0.991	1.010
	100	0.995	1.040	1.146	1.203	1.238	1.262
	120	1.193	1.248	1.375	1.443	1.486	1.515

Table 7. Simple span reduction factor for F-truck types 2D and 3 at center span.

Length (ft)	Gross Weight (kips) 10	20	40	60	80
40	0.0714	0.1171	0.2087	0.3002	0.3917
60	0.0604	0.0991	0.1766	0.2541	0.3315
80	0.0567	0.0931	0.1658	0.2386	0.3113
100	0.0551	0.0938	0.1610	0.2316	0.3022
120	0.0542	0.0890	0.1586	0.2281	0.2977
140	0.0538	0.0883	0.1573	0.2262	0.2952

Table 8. Simple span reduction factor for F-truck types 2S-1, 2S-2, and 3S-2 at center span.

Length (ft)	Gross Weight (kips) 20	40	60	80	100	120
40	0.0989	0.1512	0.2035	0.2558	0.3081	0.3604
60	0.0837	0.1279	0.1722	0.2164	0.2607	0.3050
80	0.0786	0.1201	0.1617	0.2033	0.2448	0.2864
100	0.0763	0.1166	0.1570	0.1973	0.2377	0.2780
120	0.0713	0.1149	0.1546	0.1943	0.2341	0.2738
140	0.0745	0.1139	0.1533	0.1928	0.2322	0.2716

tests, the actual stresses are increased by ($\bar{S}/5.5$), thus increasing the reduction factor F, which gives

$$F = \frac{[A + B(G)]\,L}{(9L - 140)\left(1 + \frac{50}{L + 125}\right)} \tag{4}$$

The coefficients A and B in Eq. 2 are obtained from an empirical equation, which depends on the five truck types. A close examination of these five equations (12) indicates that two equations can readily represent the response of the bridge to the five truck types. The final equation for types 2D and 3 is

$$F = \frac{[0.1835 + 0.0328\,(G)]\,L}{(9L - 140)\left(1 + \frac{50}{L + 125}\right)} \tag{5}$$

For truck types 2S-1, 2S-2, and 3S-2, the equation is

$$F = \frac{[0.3338 + 0.01874(G)]\,L}{(9L - 140)\left(1 + \frac{50}{L + 125}\right)} \tag{6}$$

The reduction factor F (Eqs. 3 and 4) is given in Tables 7 and 8 for various span lengths and gross weights. The factors give the ratios of the observed stresses to the design stresses for simple span, composite girder-slab bridges.

Off End of Cover Plate—As described for the ratio of f_{test} to f_{design} at the centerline of the structure, a similar ratio can be developed at the end of the cover plate:

$$\frac{f_{test}}{f_{design}} = \frac{A + B(G)}{S/(12L)} \times \frac{S}{M\left(\frac{\bar{S}}{5.5}\right)(1 + I)}$$

where

M = calculated moment at end of cover plate caused by a set of wheel loads of an AASHTO truck,
$\bar{S}/5.5$ = distribution factor,
$\bar{S}$ = girder spacing, and
I = impact factor = $\left(\frac{50}{L + 125}\right)$.

The AASHTO moment is determined by M_{16} kips = $16\left[(1 - N)\left(\frac{L}{2}\right)(1 + N) - 7\right]12$ kip-in. This equation was developed by positioning a set of wheel loads on an influence line diagram for moment at the cover plate of the beam shown in Figure 2. The equation for moment only contains the effect of two wheels (P = 16 kips) spaced at 14.0 ft. The 4-kip axle was assumed to be off the structure. As shown in Figure 3, the ratio of cover plate length to span length (N) is compared to span length. The limiting value of N so that the 4-kip axle remains on the girder is shown by the bound line. A plot of the data for the test bridges is also given. As can be seen, most of the bridges fall beyond the limiting N value; thus, the 4-kip load can be neglected. If the 4-kip load is to be included, the additional moment is given by the following equation: M_4 kips = $12(1 + N)$ $[L(1 - N) - 28]$ kip-in., which can then be added to the previously defined M_{16} kip equation.

Defining $F = \frac{f_{test}}{f_{design}}$ and substituting in the M_{16} kip equation into M of the general equation give

$$F = \frac{[A + B(G)]\,12L}{16\left[(1 - N)\,\frac{L}{2}(1 + N) - 7\right]12\left(\frac{\bar{S}}{5.5}\right)(1 + I)} \tag{7}$$

Figure 2. Cover-plated, simple span structure.

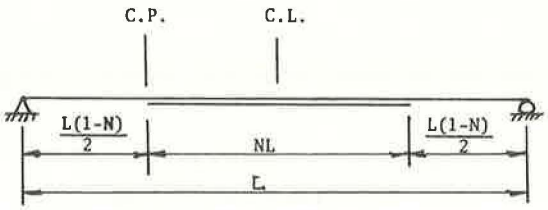

Figure 3. Span length versus fraction of cover plate length N.

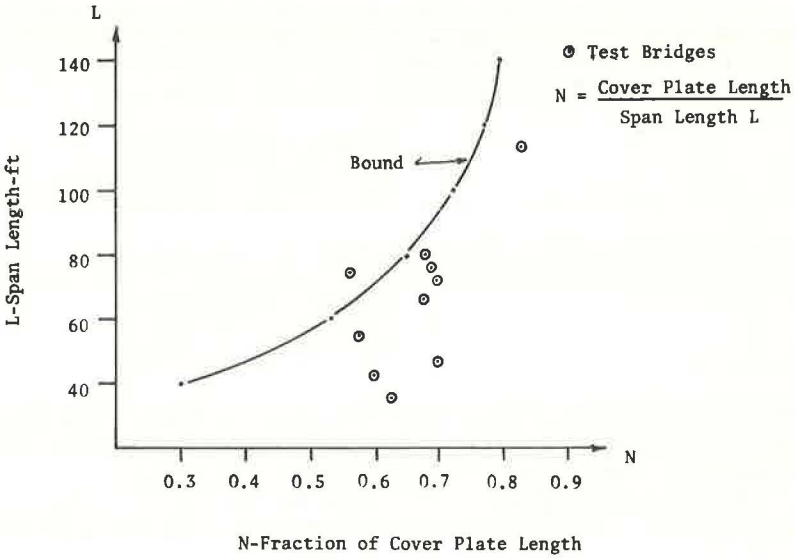

Table 9. Simple span reduction factor for F-truck types 2D and 3 at cover plate end.

N	Length (ft)	Gross Weight (kips) 10	20	40	60	80
0.50	40	0.0537	0.0954	0.1788	0.2623	0.3457
0.60	40	0.0618	0.1097	0.2057	0.3016	0.3975
0.70	40	0.0763	0.1355	0.2539	0.3724	0.4908
0.55	60	0.0534	0.0950	0.1780	0.2611	0.3441
0.60	60	0.0580	0.1030	0.1930	0.2830	0.3730
0.65	60	0.0639	0.1135	0.2128	0.3120	0.4112
0.65	80	0.0628	0.1116	0.2091	0.3067	0.4042
0.70	80	0.0707	0.1256	0.2355	0.3453	0.4551
0.75	80	0.0822	0.1460	0.2736	0.4012	0.5288
0.75	100	0.0818	0.1453	0.2724	0.3994	0.5265
0.80	100	0.0992	0.1762	0.3302	0.4843	0.6383
0.85	100	0.1284	0.2281	0.4274	0.6268	0.8262
0.80	120	0.0993	0.1764	0.3306	0.4847	0.6389
0.85	120	0.1286	0.2284	0.4280	0.6277	0.8273
0.90	120	0.1874	0.3330	0.6240	0.9151	1.2060

Table 10. Simple span reduction factor for F-truck types 2S-1, 2S-2, and 3S-2 at cover plate end.

N	Length (ft)	Gross Weight (kips) 20	40	60	80	100	120
0.50	40	0.0713	0.1223	0.1734	0.2244	0.2755	0.3265
0.60	40	0.0819	0.1407	0.1994	0.2581	0.3168	0.3755
0.70	40	0.1012	0.1736	0.2461	0.3186	0.3911	0.4636
0.55	60	0.0709	0.1218	0.1726	0.2234	0.2742	0.3250
0.60	60	0.0769	0.1320	0.1870	0.2421	0.2972	0.3523
0.65	60	0.0848	0.1455	0.2062	0.2670	0.3277	0.3884
0.65	80	0.0833	0.1430	0.2027	0.2624	0.3221	0.3818
0.70	80	0.0938	0.1610	0.2282	0.2955	0.3627	0.4299
0.75	80	0.1090	0.1871	0.2652	0.3433	0.4214	0.4995
0.75	100	0.1085	0.1863	0.2640	0.3418	0.4195	0.4973
0.80	100	0.1316	0.2258	0.3201	0.4144	0.5086	0.6029
0.85	100	0.1703	0.2923	0.4143	0.5363	0.6583	0.7803
0.80	120	0.1317	0.2261	0.3204	0.4148	0.5091	0.6035
0.65	120	0.1705	0.2927	0.4149	0.5371	0.5493	0.7814
0.90	120	0.2486	0.4268	0.6049	0.7830	0.9612	1.1390

Assume again that several trucks occur simultaneously on the bridge during the field tests. This increases the stresses by an assumed amount of ($\bar{S}$/5.5). The reduction factor is, therefore,

$$F = \frac{[A + B(G)]\,L}{16\left[(1 - N)\left(\frac{L}{2}\right)(1 + N) - 7\right]\left(1 + \frac{50}{L + 125}\right)} \tag{8}$$

A and B in Eq. 5 were obtained from a study of loading history field data (12). Data indicate that coefficients that represent the behavior of the five truck types can be reduced into two categories:

$$F = \frac{[0.0720 + 0.025(G)]\,L}{16\left[(1 - N)\left(\frac{L}{2}\right)(1 + N) - 7\right]\left(1 + \frac{50}{L + 125}\right)} \tag{9}$$

for truck types 2D and 3, and

$$F = \frac{[0.1211 + 0.0153(G)]\,L}{16\left[(1 - N)\left(\frac{L}{2}\right)(1 + N) - 7\right]\left(1 + \frac{50}{L + 125}\right)} \tag{10}$$

for truck types 2S-1, 2S-2, and 3S-2. The reduction factor F (Eqs. 6 and 7) is given in Tables 9 and 10 for various span lengths, fraction of cover plate length, and gross weights.

CONTINUOUS SPAN STUDY

M/M_A Three-Span Structure

By using the typical trucks shown in Figure 1, the maximum moments induced by these vehicles on a symmetrical two-span structure were determined. The moments in question were located at the interior support (point 1) and the midspan (point 2) of a two-span structure of length 2L. The values were then related to the AASHTO design moments as R_1 (M/M_A at interior support) and R_2 (M/M_A at midspan). The gross weights for these various truck types were assumed to be equal to the maximum values and are (a) for 2D, 50.0 kips; (b) for 3, 80.0 kips; (c) for 2S-1, 80.0 kips; (d) for 2S-2, 100.0 kips; and (e) for 3S-2, 100.0 kips. The resulting ratios for the five truck types are given in Table 11.

M/M_A Three-Span Structure

By using a similar procedure to that for a two-span structure, critical moments were evaluated in various three-span structures. The locations of the critical moments were selected at midspan of the end span (point 1, R_1); interior support (point 2, R_2); and midspan of the center span (point 3, R_3). M/M_A of the induced moments for these three points, according to the typical trucks and AASHTO loadings, are given in Tables 12 through 16 for the various truck types.

Tables 12 through 16 also give the various span lengths and the proportions of end spans to the center span. The classification of gross weights of the vehicles was assumed to be the same maximum values as those given previously.

DESIGN CRITERIA

In a general design of a bridge girder, fatigue analysis is performed after the section has been determined according to static dead- and live-load stress conditions. This fatigue analysis is based on a predetermined number of induced load applications (i.e., 100,000, 500,000, or 2,000,000 cycles) at a maximum induced stress obtained from the AASHTO truck loading. It is probably unrealistic to penalize the structure with absorption of these high stresses when it is known that the actual induced stresses

Table 11. M/M_A for two-span bridge.

Truck Type	Spans (ft)							
	80		100		120		140	
	R_1	R_2	R_1	R_2	R_1	R_2	R_1	R_2
2D	0.474	0.812	0.412	0.785	0.364	0.768	0.325	0.757
3	0.757	1.248	0.658	1.218	0.581	1.198	0.520	1.185
2S-1	0.652	0.919	0.600	0.956	0.545	0.981	0.496	1.000
2S-2	0.835	1.135	0.761	1.193	0.689	1.229	0.625	1.254
3S-2	0.811	1.121	0.747	1.177	0.680	1.214	0.619	1.240

Table 12. M/M_A for three-span bridge.

Truck Type	Midspan Length (ft)	N	R_1	R_2	R_3
2D	80	0.6	0.872	0.709	0.825
	80	0.8	0.814	0.554	0.819
	80	1.0	0.785	0.537	0.814
	100	0.6	0.824	0.623	0.795
	100	0.8	0.785	0.485	0.791
	100	1.0	0.764	0.468	0.787
	120	0.6	0.797	0.554	0.776
	120	0.8	0.767	0.430	0.772
	120	1.0	0.751	0.413	0.770
	140	0.6	0.779	0.499	0.764
	140	0.8	0.755	0.386	0.760
	140	1.0	0.742	0.370	0.758

Table 13. M/M_A for three-span bridge, truck type 3.

Truck Type	Midspan Length (ft)	N	R_1	R_2	R_3
3	80	0.6	1.313	1.132	1.257
	80	0.8	1.249	0.883	1.251
	80	1.0	1.216	0.857	1.247
	100	0.6	1.261	0.995	1.226
	100	0.8	1.216	0.774	1.221
	100	1.0	1.192	0.747	1.217
	120	0.6	1.230	0.886	1.205
	120	0.8	1.196	0.687	1.092
	120	1.0	1.177	0.661	1.198
	140	0.6	1.210	0.797	1.191
	140	0.8	1.182	0.617	1.188
	140	1.0	1.167	0.592	1.185

Table 14. M/M_A for three-span bridge, truck type 2S-1.

Truck Type	Midspan Length (ft)	N	R_1	R_2	R_3
2S-1	80	0.6	0.227	0.935	0.908
	80	0.8	0.863	0.734	0.911
	80	1.0	0.920	0.741	0.913
	100	0.6	0.843	0.884	0.942
	100	0.8	0.921	0.690	0.946
	100	1.0	0.962	0.682	0.949
	120	0.6	0.897	0.817	0.567
	120	0.8	0.957	0.635	0.883
	120	1.0	0.989	0.620	0.974
	140	0.6	0.933	0.752	0.986
	140	0.8	0.981	0.583	0.990
	140	1.0	1.007	0.565	0.993

Table 15. M/M_A for three-span bridge, truck type 2S-2.

Truck Type	Midspan Length (ft)	N	R_1	R_2	R_3
2S-2	80	0.6	0.938	1.221	1.086
	80	0.8	1.027	0.956	1.090
	80	1.0	1.112	0.944	1.093
	100	0.6	0.995	1.133	1.136
	100	0.8	1.112	0.884	1.142
	100	1.0	1.173	0.863	1.147
	120	0.6	1.075	1.038	1.174
	120	0.8	1.164	0.807	1.073
	120	1.0	1.211	0.782	1.185
	140	0.6	1.128	0.951	1.202
	140	0.8	1.199	0.737	1.208
	140	1.0	1.238	0.711	1.213

Table 16. M/M_A for three-span bridge, truck type 3S-2.

Truck Type	Midspan Length (ft)	N	R_1	R_2	R_3
3S-2	80	0.6	0.957	1.168	1.083
	80	0.8	1.035	0.916	1.091
	80	1.0	1.115	0.921	1.197
	100	0.6	1.010	1.104	1.142
	100	0.8	1.118	0.862	1.150
	100	1.0	1.175	0.850	1.156
	120	0.6	1.085	1.020	1.182
	120	0.8	1.169	0.793	1.081
	120	1.0	1.214	0.774	1.195
	140	0.6	1.137	0.939	1.211
	140	0.8	1.203	0.728	1.218
	140	1.0	1.241	0.705	1.223

Table 17. Truck distribution on three-span bridge.

Truck Type	Frequency (percent)	Trucks/Day	Trucks/Year
2D	22	220	80,500
3	10	100	36,500
2S-1	8	80	29,200
2S-2	15	150	54,800
3S-2	45	450	164,000

are much lower. The stresses that are induced also depend on the traffic characteristics; therefore, a random loading criterion appears more suitable.

Miner's Technique

Incorporation of various vehicle loading conditions, a random process, easily can be established by application of Miner's theory (13). The theory is expressed by

$$\sum\left(\frac{n_i}{N_{f_i}}\right) = 1.0 \tag{11}$$

where

n_i = number of induced cycles at a constant stress level f_i, and
N_{f_i} = number of induced cycles to institute failure at stress level f_i.

The estimated life of a structural element is then determined by solving Eq. 11:

$$N_{life} = \frac{1.0}{\sum\left(\frac{n_i}{N_{f_i}}\right)} \tag{12}$$

where $\sum\left(\frac{n_i}{N_{f_i}}\right)$ represents the damage estimate that is induced during 1 year. Therefore, a bridge could be designed in terms of years rather than cycles.

The following is the procedure for checking the fatigue life of a structural weldment:

1. Determine the probable number of trucks per day at a bridge location.
2. Determine the probable percentage of distribution of truck types at a bridge location (use Table 2 if traffic data are not available).
3. Determine the number of vehicle applications per year, i.e., percentage × daily population × 365.
4. Determine M/M_A in regard to the type of structure, vehicle type, and vehicle gross weight (Tables 5 and 10 through 15).
5. Modify AASHTO design live-load stress according to percentage of M/M_A—$f_i = f_{design} \times M/M_A$—for each truck type.
6. Determine the failure cycles at the induced stress f_i for the given truck type, where the failure cycles N_{f_i} are computed from the following equations (11):

$$\log N_{f_i} = 8.87 - 2.65 \log f_i \tag{13}$$

for cover-plated beams, and

$$\log N_{f_i} = 10.637 - 2.94 \log f_i \tag{14}$$

for plain and butt-welded beams.

7. Compute the estimated life of structure in relation to each of the five truck types by using Eq. 12.
8. Determine whether this estimated life is satisfactory.

Root-Mean-Square Technique

As an alternate to Miner's procedure, the influence of the five truck types can be combined into one common denominator by evaluating the root-mean-square (rms) of their stresses (14). This stress is then used to evaluate the fatigue life.

The general equation used for determining rms stress is

$$f_{rms} = \{[(f_{2D})^2 + (f_3)^2 + (f_{2S-1})^2 + (f_{2S-2})^2 + (f_{3S-2})^2]/5.0\}^{1/2} \tag{15}$$

where f_{2D}, f_3, f_{2S-1}, f_{2S-2}, and f_{3S-2} = stresses induced by 2D, 3, 2S-1, 2S-2, and 3S-2 truck types respectively.

The following procedure is used for checking the fatigue life of a structural weldment with the rms technique:

1. Determine the probable number of trucks per day at bridge location.
2. Determine the number of vehicle applications per year, i.e., daily population (DP) × 365.
3. Determine M/M_A in regard to the type of structure, vehicle type, and vehicle gross weight (Tables 5 and 10 through 15).
4. Modify AASHTO design live-load stress according to percentage of M/M_A—$f_1 = (f)_{design} \times M/M_A$—for each truck type.
5. Use computed stresses f_1, for each of the five truck types, to compute f_{rms} as given by Eq. 15.
6. Determine failure cycles N_f at the f_{rms} stress level by using Eqs. 13 and 14.
7. Compute estimated life of structure, i.e., $N_{years} = \frac{N_{f_{cycles}}}{365 \times DP}$.
8. Determine whether this estimated life is satisfactory.

The reduction factors given in Tables 7 through 10 were not listed as part of the design procedure. These factors can be used with modifying factors to obtain a more realistic estimate of the actual induced stress. Therefore, the final stress f_1 is computed as

$$f_1 = f_{design} \times M/M_A \times F \tag{16}$$

If a conservative estimate is required, F = 1.0 would be used.

APPLICATION

Examination of truck classification data (5, 6) and a load history study of a three-span continuous bridge yielded the truck distributions given in Table 17. (The average daily traffic was 1,000 trucks. The values for the number of trucks per day times 365 equals the trucks per year.)

The bridge to be examined under these loadings (Table 17) has three spans: 72, 90, and 72 ft long (Fig. 4). The bridge is composite in the positive moment region and has a 7-in. concrete slab. The girders are spaced at 7-ft, 7-in. intervals. The section properties of a typical interior girder at sections A, B, and C and the design live-load moments and stresses are given in Table 18. With this information, the induced stresses caused by the five truck types can now be determined.

Tables 12 through 16 are used. It will be assumed that the center span is 100 ft (90 ft actually) and the end span ratio equals 72/90 or 0.80.

The induced stresses caused by the five truck types are computed by multiplying the design stresses by the M/M_A factors. These stresses must also reflect the passage of a single vehicle rather than all lanes loaded as is assumed in the original design. This can be achieved by using a new distribution factor of S/11.0 (15). Thus a ratio of S/11.0 to the AASHTO distribution factor S/5.5 gives a factor of 0.50. Therefore, the resulting stresses caused by the various truck types (Table 19) are computed as

$$\text{Stress}_{\text{truck type}} = (\text{design stress})\left(\frac{M}{M_A}\right)\left(\frac{S/11.0}{S/5.5}\right)$$

The rms stress for $R_1 = 5.95$, for $R_2 = 3.37$, and for $R_3 = 6.15$.

The fatigue life of a plain or butt-welded girder subjected to these stresses is obtained by Eq. 14. The stresses at midspan of the center girder will govern. The cycles to failure ($N_f \times 10^6$) are given in Table 20 (rms = 209.2). These resulting N_f values and the frequencies of applied stresses per truck type will now be used to determine the estimated failure life with Miner's and the rms techniques.

Miner's Technique

The damage index is n_i/N_{f_i} and is given in Table 21. The estimated life is the reverse of n_i/N_{f_i} or

Figure 4. Three-span continuous bridge.

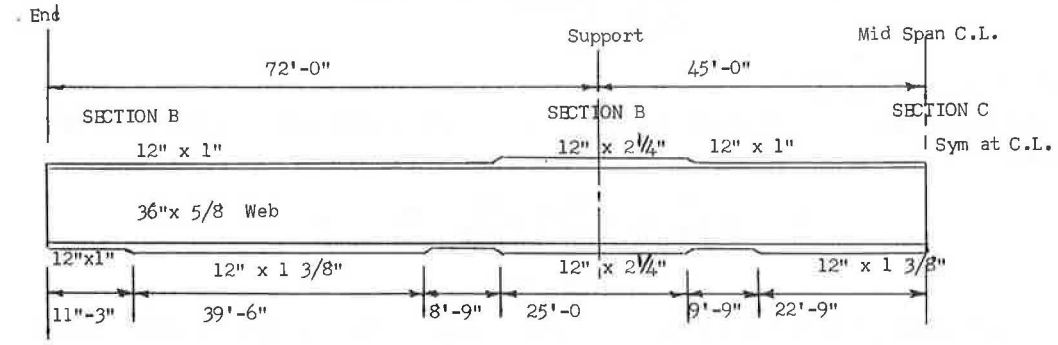

Table 18. Interior girder descriptions for a three-span continuous bridge.

Section	Type	Section Modulus ($in.^3$)	Design Moment (kip-ft)	Stress (ksi)
A, support	Noncontinuous	849.0	-635.0	-9.0
B, endspan	Continuous	739.0	690.0	11.37
C, midspan	Continuous	739.0	716.0	11.59

Table 19. Stresses caused by various truck types.

Truck Type	Stress (ksi) R_1 (end span)	R_2 (support)	R_3 (midspan)
2D	4.47	2.67	4.57
3	6.95	3.48	7.05
2S-1	5.25	3.10	5.50
2S-2	6.30	3.97	6.60
3S-2	6.35	3.89	6.65

Table 20. Cycles to failure.

Truck Type	Cycles to Failure at R_3 (midspan)
2D	501.0
3	140.1
2S-1	290.6
2S-2	170.1
3S-2	166.3

Table 21. Damage index.

Truck Type	$n_i \times 10^3$	n_i/N_f
2D	80.5	0.000161
3	36.5	0.000261
2S-1	29.2	0.000100
2S-2	54.8	0.000320
3S-3	164.0	0.000990

$$N_{life} = \frac{1}{\sum \frac{n_i}{N_{f_i}}} = \frac{1}{0.00183} = 546 \text{ years}$$

Root-Mean-Square Technique

The estimated bridge life is computed from the rms failure life of $N_f = 209.2 \times 10^6$ cycles:

$$N_{life} = \frac{N_f}{365 \times DP} = \frac{209.2 \times 10^6}{365 \times 1{,}000} = 574 \text{ years}$$

CONCLUSION

A methodology has been presented by which random truck loading on a bridge can be considered relative to the fatigue response of welded plate elements.

Examination of field data, as reported by various states, has resulted in a series of typical trucks that were used as loads in evaluating induced girder moments. The induced field stresses were compared to the calculated stresses, and this resulted in the determination of reduction factors. These factors may be used to modify design stresses.

Further studies should be conducted in developing accurate single-vehicle load distribution factors S/11.0. The tables also should be refined to reflect other moment locations along the girders. The suggested fatigue design procedure is derived from field tests on multiple beam and slab bridges and, therefore, should only be used on similar structures.

ACKNOWLEDGMENTS

The data obtained from this study were gathered as part of a project sponsored by the Maryland Department of Transportation and the Federal Highway Administration. Their cooperation and encouragement are gratefully acknowledged.

REFERENCES

1. Douglas, T. R. Fatigue of Bridges Under Repeated Highway Loadings. Civil Engineering Dept., Univ. of Alabama, Rept. 54, April 1971.
2. Bowers, D. G. Loading History, Span No. 10 Yellow Mill Pond Bridge, I-95, Bridgeport, Connecticut. Connecticut Department of Transportation, May 1972.
3. Christiano, P., Goodman, L. E., and Sun, C. N. Bridge Stress Range History and Diaphragm Stiffening Investigation. Civil Engineering Dept., Univ. of Minnesota, April 1970.
4. Heins, C. P., and Sartwell, A. D. Tabulation of 24 Hour Dynamic Strain Data on Four Simple Span Girder-Slab Bridge Structures. Civil Engineering Dept., Univ. of Maryland, Rept. 29, June 1969.
5. Sartwell, A. D., and Heins, C. P. Tabulation of Dynamic Strain Data on a Girder Slab Bridge Structure During Seven Continuous Days. Civil Engineering Dept., Univ. of Maryland, Rept. 31, Sept. 1969.
6. Sartwell, A. D., and Heins, C. P. Tabulation of Dynamic Strain Data on a Three Span Continuous Bridge Structure. Civil Engineering Dept., Univ. of Maryland, Rept. 33, Nov. 1969.
7. Galambos, C. F., and Heins, C. P. Loading History of a Highway Bridge—Comparison of Stress Range Histograms. Public Roads Journal, Vol. 36, No. 9, Aug. 1971.
8. Desrosiers, R. D. The Development of a Technique for Determining the Magnitude and Frequency of Truck Loadings on Bridges. Civil Engineering Dept., Univ. of Maryland, Rept. 24, April 1969.
9. Cudneg, G. R. The Effects of Loadings on Bridge Life. Department of State Highways, State of Michigan, Sept. 1967.
10. McKeel, W. T., Maddox, C. F., Kinnier, H. L., and Galambos, C. F. A Loading History Study of Two Highway Bridges in Virginia. Virginia Highway Research Council, Charlottesville, Dec. 1971.

11. Fisher, J. W., Frank, K. H., Hirt, M. A., and McNamee, B. M. Effect of Weldments on the Fatigue Strength of Steel Beams. NCHRP Rept. 102, 1970.
12. Khosa, R. L., and Heins, C. P. Study of Truck Weights and the Corresponding Induced Bridge Girder Stresses. Civil Engineering Dept., Univ. of Maryland, Rept. 40, Feb. 1971.
13. Miner, M. A. Cumulative Damage in Fatigue. Jour. Applied Mechanics, Vol. 12, No. 1, Sept. 1945.
14. Swanson, S. R. Random Load Fatigue Testing: A State of the Art Survey. Materials Research and Standards, Vol. 8, No. 4, ASTM, Philadelphia, April 1968.
15. Heins, C. P., Jr., and Forbes, R. Analysis Charts for Issuing Vehicle Permits. Published in this RECORD.

NEW PROCEDURE FOR FATIGUE DESIGN OF HIGHWAY BRIDGE GIRDERS

Fred Moses, Civil Engineering Department, Case Western Reserve University; and Robert Garson, Massachusetts Institute of Technology

The wide variety of heavy truck traffic and bridge girder weld conditions combined with reported low measured stress levels under random traffic suggests there must currently be inconsistent safety margins against bridge fatigue. This paper discusses a probabilistic load model that forecasts histograms of highway bridge loading and that can be used to predict fatigue life and to properly size girder sections. A reliability or risk approach to choosing safety factors on material and load is also described. The simplified design procedure based on the truck loading model permits cross sections to be designed or checked against fatigue by a simple formula that also includes as parameters truck volume, span length, weld category, and location.

•CONSIDERABLE attention has been devoted recently to the possibility of fatigue failure in steel girder highway bridges. Field measurement studies under actual random traffic conditions have been made in several states (1). These tests have shown that in most cases actual stress histories experienced by bridge girders are considerably below the allowable AASHTO code standards. This is partly because fatigue is treated in the AASHTO code as a byproduct of the yield or overload analysis, which requires high distribution factors, all lanes loaded, conservative truck weights and dimensions, and so on.

In introducing higher strength steels, continuous spans, and welding details, fatigue often controls the required girder size. In view of the low measured stresses, modifications in the current specification appear appropriate. The current code also does not distinguish between the wide range encountered in both gross truck weight distributions and annual truck volumes. Although the AASHTO code suggests you may do otherwise, based on traffic and loadometer surveys (2), it does not offer any alternatives. This paper presents a detailed procedure for fatigue life design that incorporates these factors and illustrates it with several examples.

A further indication of the need for design changes is that many specifications are evolving toward a probabilistic basis for choosing safety factors. One common example is separate or split safety factors on load and strength. This paper also illustrates how this can be done for the fatigue design problem. A material safety factor is introduced to account for fatigue life variabilities, and a second safety factor on load is used to account for uncertainties in future load growth and possible errors in analysis.

FATIGUE LIFE ANALYSIS PROCEDURE

A new fatigue code format that is based on a more realistic evaluation of fatigue loading and material properties and yet can be simplified enough for practical design is discussed. The goal of the fatigue life analysis procedure was to incorporate field measurements, laboratory data, and state records of truck weights and volumes so they could be used for evaluating and predicting girder fatigue life (3).

Publication of this paper sponsored by Committee on Dynamics of Field Testing of Bridges.

In the fatigue prediction calculations (3), it was found that two truck types, including single and tractor-trailer vehicles, would sufficiently represent all bridge truck loadings. The truck physical parameters were defined from a survey of actual data rather than from extremely unfavorable cases as in the yield design provisions of the AASHTO code. For a particular roadway type and location, a local gross weight distribution and percent by volume of each truck type based on state records were used.

By using a static analysis of the bridge girders, the live-load bending moment range at any point along the girder was found for both truck types. From these static analyses, a computer program calculated the bending moment range histogram for the critical bridge location. The flow chart of fatigue calculations is shown in Figure 1. The bending moment also includes a dynamic impact factor that increases the maximum moment and decreases the minimum value and thereby considerably raises the moment range. This is handled in the program by calculating an envelope of the moment pulse as the truck moves across the bridge. The analytical model of truck loadings also included a truck headway distribution for the important effects of truck loading superpositions caused by closely spaced trucks or trucks passing each other.

These calculated moment histograms have compared favorably to histograms of field measurements. It must be emphasized that the computer program is only used to develop a set of tabulated parameters in a specification, but it is not needed for everyday design or checking cross sections. (This is illustrated below in a simplified design procedure.) The calculations also showed that it was sufficient to consider the fatigue life at some critical location such as the span center on some representative bridge length, and for any other span location and length the results could be directly extrapolated by computing static moment ranges based on a tractor-trailer vehicle. The basic idea is that fatigue damage depends on the stress range experienced by an element and that the tractor-trailer loading is sufficiently representative for comparing locations.

The computed bending moment histogram is then converted to a stress histogram by dividing moment by an equivalent elastic girder section modulus Z_{eq}. The fatigue life is computed by Miner's damage rule in which each stress range level causes damage in inverse proportion to the fatigue life for that stress level. Because only one constant, Z_{eq}, is needed to relate loading to stress, it becomes convenient to determine fatigue life versus Z_{eq} for a given truck volume. Thus, the loading information is contained in the bending moment histogram, whereas Z_{eq} contains all the information on the bridge girder section. This calculation uses the result of Fisher, Frank, Hirt, and McNamee (4) that only live-load stress range and not dead load affects fatigue life. Figure 2 shows a plot of truck volume versus Z_{eq} for different design lives based on a moment histogram calculated from a representative sampling of Ohio truck weight records (5).

The fatigue checking and design method, however, does not require in each case a computer for calculating bending moments and fatigue damage. A literature survey of fatigue information showed that the fatigue S-N curve or stress range versus the number of cycles to failure is a straight line on log-log paper with essentially the same slope regardless of steel or weld type. This assumption permits extrapolating both weld category and a safety or risk factor without further recalculation of bending moments. The weld category is treated by a single term D_f that, like an equivalent stress concentration factor, moves the fatigue curve parallel to itself (Fig. 1). The same holds for the material safety factor N_s, which can be treated as a risk value inasmuch as safety factors greater than 1 correspond to definable risk levels such as $1/100$ or $1/1,000$ of a fatigue failure during the girder lifetime (3). The various factors are summarized in the following equations.

The uniform amplitude fatigue curve is

$$NS^b = c \tag{1}$$

where

N = number of cycles to failure;
S = uniform amplitude stress;

Figure 1. Flow diagram of fatigue evaluation.

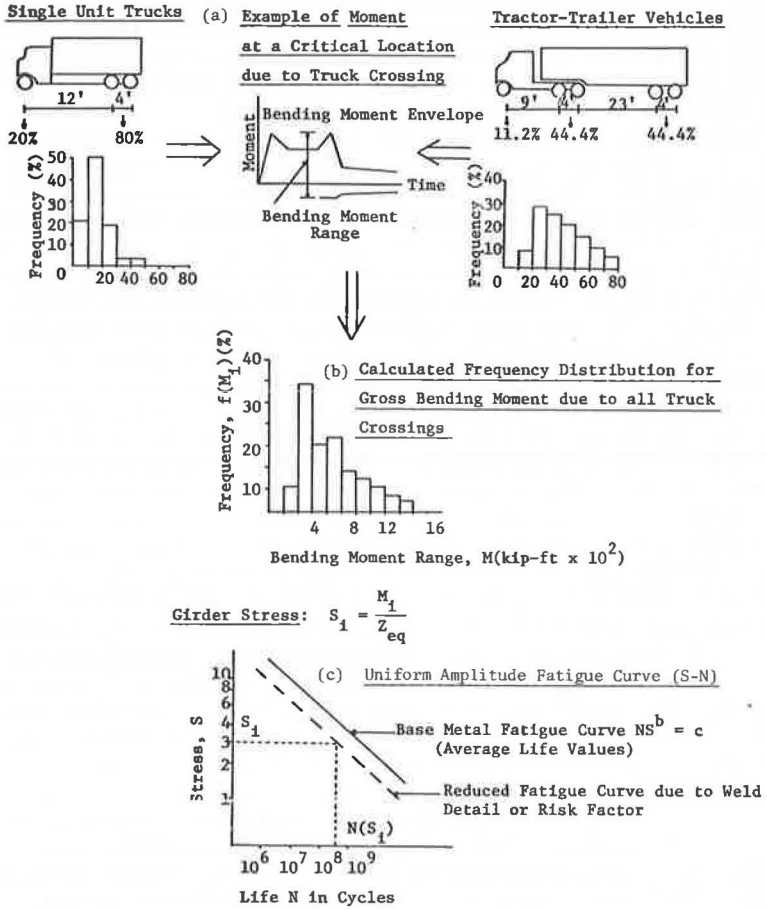

(d) Life Prediction: Damage, $D = V\Sigma D_1 = \frac{V}{c}\Sigma S_1^b f(M_1) = \frac{V}{Z_{eq}^b c}\Sigma M_1^b f(M_1)$

$$\text{Life} = \frac{1}{D}, \text{ years}$$

b = fatigue slope, equal to about 3 in all cases; and
c = constant.

The fatigue damage D_i by Miner's criterion for a single application of stress range S_i is

$$D_i = \frac{1}{N(S_i)} \tag{2}$$

where

$$N(S_i) = \frac{c}{S_i^b}$$

The cumulative damage D may be found from the computed histogram of bending moments:

$$D = \sum D_i = V \sum \frac{f(M_i)}{N(S_i)} = \frac{V}{c} \sum S_i^b f(M_i) \tag{3}$$

where

V = truck volume, and
$f(M_i)$ = frequency or percentage of live-load bending moment ranges equal to M_i from the calculated moment histogram.

The stress is assumed to be moment M_i divided by an equivalent elastic section modulus Z_{eq} or

$$S_i = M_i/Z_{eq} \tag{4}$$

Substituting Eqs. 2 and 4 into Eq. 3 gives

$$D = \frac{V}{Z_{eq}^b c} \sum M_i^b f(M_i) \tag{5}$$

Failure occurs by Miner's law when D, the cumulative damage, equals 1. Note that the loading terms are incorporated in the moment frequency inside the sum in Eq. 5, whereas the fatigue category, girder properties, and truck volume are outside the sum and can be incorporated in the constant Z_{eq}. [In Moses and Garson (3) Z_{eq} appears as DR (design ratio), i.e., $1/Z_{eq}$.] A general expression for Z_{eq} is

$$Z_{eq} = \frac{ZD_f}{GN_n N_L} \tag{6}$$

The variables in Eq. 6 are as follows:

1. G is the distribution factor expressed as the percentage of the total live-load truck bending moment on the bridge as the truck goes to an individual girder. Based on some reported field measurements of random traffic, G equals about S'/25 (3).
2. S' is the girder spacing in feet.
3. N_n is the safety or risk factor. A review of fatigue life variabilities in tests showed that a value of 1.75 would seem equal to risks less than one fatigue failure that occurs in the expected life of 10,000 bridges (3). Some results of laboratory fatigue tests tend to show that fatigue life has a log normal distribution. Thus, equal probability fatigue curves (P-S-N lines) would plot on a log-log S-N diagram as a series of straight lines. This enables the risk or safety factor to be reflected as a single constant value S_f at all stress levels.
4. Z is the girder section modulus, in in.^{3}.
5. D_f is the weld category factor that is analogous to a stress concentration (ratio of fatigue curve stress intercept to fatigue intercept for cover plate determination).

Table 1 gives some suggested values for various weld categories based primarily on lab tests (4). Because the value of c in Eq. 1 is also needed to compute fatigue damage, the weld category values are given as ratios of the value for a cover plate termination.

6. N_L is the load factor to account for future truck growth in volume and gross weight distribution as well as any errors in stress analysis and impact factor. A value of 1.5 was used. [Some studies of load growth show mean weights increasing 2.5 percent per year (3).]

Because the value of Z_{eq} is fixed by Eq. 5 for a given loading and fatigue life, a simplified design procedure uses values of Z_{eq} for different roadway categories and locations. For example, combining gross weight data from 12 rural Ohio locations (5) to determine weight distribution for calculating the bending moment histogram gave a value of Z_{eq} equal to 1,700 in.^{3} for a 100-year life, 36 trucks per hour, and the center of a 60-ft simple span girder. On some Maryland weight records (6) Z_{eq} was 1,333 in.^{3} for the same life and bridge. These values of Z_{eq} should be taken only as illustrative because they were based on very selective locations. Further study of weight records will be needed. However, only truck weight distribution must be considered as span; volume and life factor out.

FATIGUE DESIGN PROCEDURE

The following steps are required by the suggested fatigue design procedure.

Select the section modulus value Z_{eq} now designated as $(Z_{eq})_{tab}$ for the roadway category into which the design location is expected to fall. The tabulated values besides the truck weight characteristics are based on specified truck volume, bridge length, impact factor, and location of critical weld. Adjustments to account for these quantities follow.

Adjust the value of Z_{eq} by any change in the desired service life and expected traffic volume (Eq. 5) so that it has the same fatigue damage. The section modulus Z_{eq} and volume V must satisfy the formula

$$\frac{V}{Z_{eq}^b} = \text{constant} \tag{7}$$

If V is the truck volume used to calculate the tabulated value of Z_{eq}, then the modified Z_{eq} for another truck volume, V, would be

$$Z_{eq} = (Z_{eq})_{tab}\left(\frac{V}{V_{tab}}\right)^{1/b} \tag{8}$$

where V is the actual truck volume expected at the site, and V_{tab} is fixed (e.g., 36 trucks per hour for a 100-year life).

Select, from a structural analysis, coefficients for the location of the critical cross section and span length, and adjust for any differences in impact factor. These coefficients are

$$Z_{eq} = \frac{(Z_{eq})_{tab}}{C_{XL}C_I} \tag{9}$$

where the variables C_{XL} and C_I are as follows:

1. C_{XL} is the ratio of bending moment range, found by using a tractor-trailer vehicle for the design section, to the bending moment range used in calculating $(Z_{eq})_{tab}$ values. In the examples, this was based on the center of a 60-ft span. Table 2 gives C_{XL} values for various simple span lengths and locations.

2. C_I is based on the ratio of the expected impact factor to the value used to calculate the $(Z_{eq})_{tab}$ values. The impact factor used to calculate the damage was arbitrarily taken as 20 percent. Thus, if any other impact value I is used then

Figure 2. Z_{eq} versus truck volume and design life.

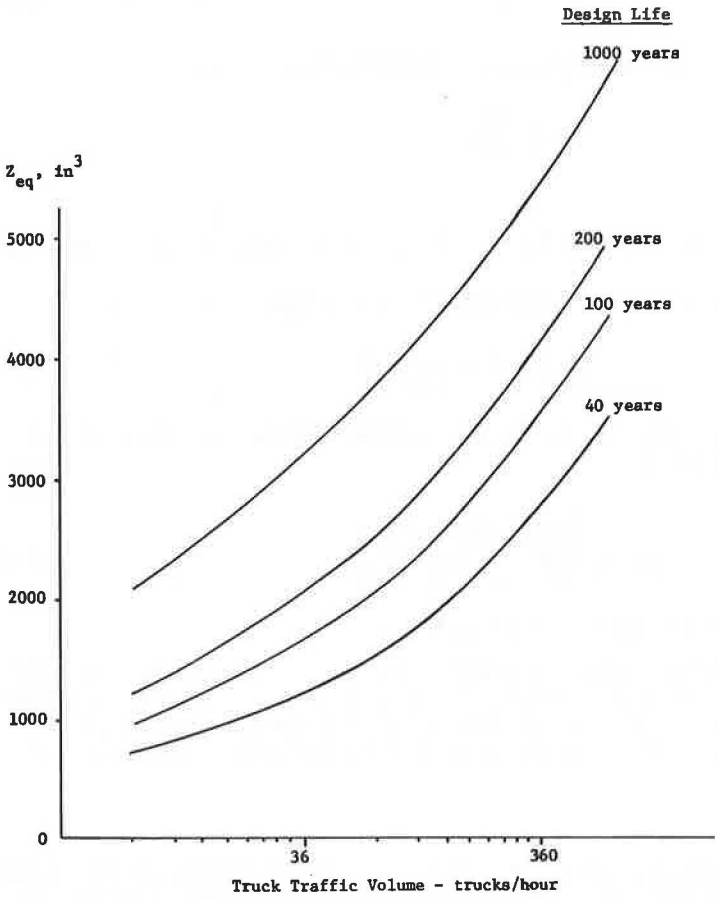

Table 1. Suggested design detail factors (D_f).

Design Factor	Detail
3.56	Rolled sections
2.58	Welded beams and girders
2.22	Welded flange splices
1.00	Cover plate terminations

Table 2. C_{XL} values for various simple span lengths and locations.

Length (ft)	Weld Location				
	2/10	3/10	5/10	7/10	8/10
20	6.16	4.88	4.38	4.88	6.27
30	3.59	2.83	2.50	3.08	3.98
40	2.56	1.98	1.72	2.20	2.78
50	1.87	1.52	1.31	1.48	1.87
60	1.37	1.10	1.00	1.05	1.37
70	1.07	0.85	0.758	0.820	1.07
80	0.873	0.69	0.606	0.672	0.873
90	0.740	0.581	0.508	0.566	0.740
100	0.642	0.503	0.436	0.491	0.642
110	0.565	0.442	0.382	0.433	0.565
120	0.508	0.394	0.340	0.388	0.508

$$C_I = \frac{1.2}{I} \tag{10}$$

where I is the impact factor. For example, if the AASHTO value is used

$$I = 1 + \frac{50}{L + 125}$$

where L is span length.

Choose a stringer spacing S′ and weld detail. Table 1 gives values of D_f for various weld details.

Calculate the required girder section modulus Z by using Eqs. 6, 8, and 9.

$$Z = (Z_{eq})_{tab} \frac{GN_B N_L}{D_f \cdot C_{XL} \cdot C_I} \left(\frac{V}{V_{tab}}\right)^{1/6} \tag{11}$$

A general equation for checking the elastic section modulus in terms of truck volume and bridge and weld characteristics is

$$Z = (Z_{eq})_{tab} \frac{\left(\frac{S'}{25}\right)(1.75)(1.5)}{D_f \cdot C_{XL} \cdot C_I} \left(\frac{V}{36}\right)^{1/3} \tag{12}$$

EXAMPLES OF FATIGUE DESIGN

Several examples illustrate the simplified fatigue design procedure described. The examples are not inclusive, and an extensive study needs to be taken of (a) truck weight variations at different locations, (b) a larger range of continuous span bridges, and (c) additional weld categories. However, all elements of the design procedure are indicated.

Example 1

Example 1 is a 60-ft simple span with a Maryland truck weight histogram (6). It has a 100-year service design with 36 trucks per hour expected volume. The design calls for a rolled beam on 7-ft center spacings. Z_{eq} for this truck weight histogram was 1,333 in.^{3}. The impact factor by the AASHTO code is I = 1 + [50/(60 ft + 125)] = 1.27. Therefore, C_I = 1.2/1.27 = 0.95. For a rolled beam, Table 1 gives D_f = 3.56. Table 2 gives C_{XL} equal to 1.0 for this case. Substituting in Eq. 12 gives, for the required girder section modulus,

$$Z = 1{,}333 \frac{\left(\frac{7\text{ ft}}{25}\right)(1.75)(1.5)}{(3.56)(1.0)(0.95)} = 293 \text{ in.}^3 \tag{13}$$

Example 2

Example 2 has the same bridge data and truck volume as in example 1 except the truck weight histogram is from Ohio (5). Z_{eq} for this case was 1,700 in.^{3}; thus,

$$Z = 1{,}700 \frac{\left(\frac{7\text{ ft}}{25}\right)(1.75)(1.5)}{(3.56)(1.0)(0.95)} = 293 \times \frac{1{,}700}{1{,}333} = 375 \text{ in.}^3 \tag{14}$$

Example 3

Example 3 has the same data as example 1, but plate girders with twice the spacing (14 ft) rather than rolled beams were used. Table 1 gives D_f = 2.58 for a welded plate girder. The section modulus now required is

$$Z = 1{,}333 \frac{\left(\frac{14}{25}\right)(1.75)(1.5)}{(2.58)(1.0)(0.95)} = 2 \times \frac{3.56}{2.58} \times 293 = 815 \text{ in.}^3 \quad (15)$$

Example 4

Example 4 is a simple span bridge with the same data as example 1, but a rolled beam with cover plate at 2/10 span is used with a spacing of 7 ft, 11 in. In this case both the section at midspan and the section at the weld cutoff must be checked. Table 1 gives a value of $D_f = 1.0$ for a cover plate termination and 2.58 for a welded beam at the midspan. Table 2 gives the value of 1.37 for C_{xL} at the weld cutoff. Thus,

$$Z_{midspan} = 1{,}333 \frac{\left(\frac{7^{11}/_{12}}{25}\right)(1.75)(1.5)}{(2.58)(1.0)(0.95)} = 455 \text{ in.}^3$$

$$Z_{2/10cutoff} = 1{,}333 \frac{\left(\frac{7^{11}/_{12}}{25}\right)(1.75)(1.5)}{(1.0)(1.37)(0.95)} = 850 \text{ in.}^3 \quad (16)$$

Example 5

Example 5 has the same data as example 1 but has a change in truck rate from 36 trucks per hour to 100 trucks per hour (100-year life). With Eq. 8, Z_{eq} is modified by

$$Z_{eq} = (Z_{eq})_{tab} \left(\frac{100}{36}\right)^{1/6} = 1{,}333 \times (2.78)^{1/6} = 1{,}800 \text{ in.}^3$$

and

$$Z = 293 \left(\frac{1{,}800}{1{,}333}\right) = 413 \text{ in.}^3 \quad (17)$$

Example 6

Example 6 has the same data as example 1 but has an 80-ft bridge instead of a 60-ft bridge. The impact factor should be modified because the computed Z_{eq} value is based on 1.2 rather than on AASHTO values. By using Eq. 10

$$C_I = \frac{1.2}{1 + \frac{50}{80 + 125}} = 0.96$$

For 80 ft and a midspan location, $C_{xL} = 0.606$ (Table 2). Z_{eq} is now modified by these values with Eqs. 9 and 10:

$$Z_{eq} = \frac{1{,}333}{(0.606)(0.96)} = 2{,}300 \text{ in.}^3$$

and the required girder section modulus

$$Z = \frac{2{,}300}{1{,}333} \times 293 = 502 \text{ in.}^3 \quad (18)$$

Example 7

A three-span bridge located in Portage County, Ohio, was used and will be checked for adequate section modulus by the procedures presented. The cross section consisted of 36 W 150 beams ($Z = 504$ in.^{3}) at 7-ft, 11-in. spacing with cover plates at the supports. The symmetric three spans are 48, 60, and 48 ft with cover plates extending

6 ft on either side of the intermediate supports. The truck rate is 70 trucks per hour.

Fatigue checks will be done at A, center of first span; B, center of middle span; and C, cover plate termination location in first span.

A static bending moment analysis is done by using influence functions, and a tractor-trailer loading gave the following $C_{\chi L}$ values based on the ratio of peak bending moment range to the center moment on a 60-ft simple span. At A, $C_{\chi L} = 1.25$; at B, $C_{\chi L} = 1.38$; and at C, $C_{\chi L} = 2.15$. A dynamic analysis gave an impact factor ratio value of C_I of about 0.94 applicable at all three locations. The detail factor at A and B is 3.56 for a rolled beam and 1.0 at C for a cover plate termination. Assuming the Ohio weight histogram (5), which would seem applicable at site, Z_{eq} was given above as 1,700 in.^{3} based on 36 trucks per hour. Thus, from Eq. 8:

$$Z_{eq} = (Z_{eq})_{tab}\left(\frac{70}{36}\right)^{1/5} = (1{,}700)(1.94)^{1/5} = 2{,}120 \text{ in.}^3$$

Substituting now for the required section modulus expression (Eq. 12) gives

$$Z_A = 2{,}120\,\frac{\left(\frac{7^{11}/_{12}}{25}\right)(1.75)(1.5)}{(3.56)(1.25)(0.94)} = 423 \text{ in.}^3 \quad (<504)$$

$$Z_B = 2{,}120\,\frac{\left(\frac{7^{11}/_{12}}{25}\right)(1.75)(1.5)}{(3.56)(1.38)(0.94)} = 385 \text{ in.}^3 \quad (<504)$$

$$Z_C = 2{,}120\,\frac{\left(\frac{7^{11}/_{12}}{25}\right)(1.75)(1.5)}{(1.0)(2.15)(0.94)} = 870 \text{ in.}^3 \quad (>504) \qquad (19)$$

Because the actual section has a modulus of 504 in.^{3}, locations A and B are satisfactory although C is relatively unsatisfactory. (Fatigue checks should also be done at the pier.) It should be emphasized that the above checks on section size reflect the assumed values of risk N_R (1.75), the load factor N_L (1.5), and a truck weight histogram averaged from several locations.

CONCLUSIONS

The study confirmed changes generally needed in fatigue specification, i.e., a fatigue loading separate from yield loading, consideration of live-load stress range rather than maximum peak stress, and updating of the load analysis to reflect actual traffic and truck load conditions on a given roadway.

Further effort is needed to clarify several points. These include continuous span bridges (only a three-span has been done thus far), the number of roadway types with different gross weight distributions and type percentages, the girder distribution and detail factors, and the material and load safety factors. These must be found from further field and laboratory measurements and calibration with existing designs.

ACKNOWLEDGMENTS

The investigation was performed in the Division of Solid Mechanics, Structures, and Mechanical Design at Case Western Reserve University under the sponsorship of the Ohio Department of Transportation and the Federal Highway Administration. The support, cooperation, and assistance given by these organizations are gratefully acknowledged. However, the opinions, findings, and conclusions expressed in this paper are those of the authors and not necessarily those of the Ohio Department of Transportation or the Federal Highway Administration.

REFERENCES

1. Heins, C. P., and Golombos, C. F. Highway Bridge Fatigue Tests in the United States, 1948-1970. Public Roads, Vol. 36, No. 12, Feb. 1972.
2. Standard Specifications for Highway Bridges. AASHO, Washington, D.C., 1969.
3. Moses, F., and Garson, R. C. Probability Theory for Highway Bridge Fatigue Stresses. Case Western Reserve Univ. for Ohio Dept. of Transportation, Final Rept., July 1973.
4. Fisher, J. W., Frank, K. H., Hirt, M. A., and McNamee, B. M. Effect of Weldments on the Fatigue Strength of Steel Beams. NCRHP Rept. 102, 1970.
5. Ohio Department of Highways Loadometer Study—1968. Division of Planning and Programming, Bureau of Planning Survey, Ohio Dept. of Highways.
6. Novak, M. E., Heins, C. P., and Looney, C. T. G. Induced Dynamic Strains in Bridge Structures due to Random Truck Loadings. Civil Engineering Dept., Univ. of Maryland, Feb. 1968.

SPONSORSHIP OF THIS RECORD

GROUP 2—DESIGN AND CONSTRUCTION OF TRANSPORTATION FACILITIES
W. B. Drake, Kentucky Department of Transportation, chairman

STRUCTURES SECTION
Arthur L. Elliott, California Division of Highways, chairman

Committee on General Structures
W. J. Wilkes, Federal Highway Administration, chairman
William L. Armstrong, N. H. Bettigole, Martin P. Burke, Jr., Daniel E. Czernik, Arthur L. Elliott, Donald C. Frederickson, George G. Goble, William A. Kline, Heinz P. Koretzky, Robert M. Olson, Adrian Pauw, Frank D. Sears, Wendell M. Smith

Committee on Dynamics and Field Testing of Bridges
Robert F. Varney, Federal Highway Administration, chairman
James W. Baldwin, Jr., Edwin G. Burdette, Paul F. Csagoly, Michael E. Fiore, Charles F. Galambos, Egbert R. Hardesty, Conrad P. Heins, Jr., Cornie L. Hulsbos, Henry L. Kinnier, Kenneth H. Lenzen, Norman G. Marks, Fred Moses, W. H. Munse, Leroy T. Oehler, Frederick H. Ray, Ronald R. Salmons, W. W. Sanders, Jr., Chester P. Siess, William H. Walker, Robert K. L. Wen, G. W. Zuurbier

Lawrence F. Spaine, Transportation Research Board staff

Sponsorship is indicated by a footnote on the first page of each report. The organizational units and the chairmen and members are as of December 31, 1973.